

# THE IDENTIFICATION OF RR LYRAE AND $\delta$ SCUTI STARS FROM VARIABLE *GALEX* ULTRAVIOLET SOURCES.

T.D. KINMAN<sup>1</sup>

National Optical Astronomy Observatory, 950 N. Cherry Avenue, Tucson, AZ 85719, USA

WARREN R. BROWN

Smithsonian Astrophysical Observatory, 60 Garden St., Cambridge, MA 02138, USA

*AJ accepted*

## ABSTRACT

We identify the RR Lyrae and  $\delta$  Scuti stars in three catalogs of *GALEX* variable sources. The *NUV* amplitude of RR Lyrae stars is about twice that in *V*, so we find a larger percentage of low amplitude variables than catalogs such as Abbas et al. (2014). Interestingly, the  $(NUV - V)_0$  color is sensitive to metallicity and can be used to distinguish between variables of the same period but differing  $[Fe/H]$ . This color is also more sensitive to  $T_{eff}$  than optical colors and can be used to identify the red edge of the instability gap. We find 8  $\delta$  Scuti stars, 17 RRc stars, 1 RRd star and 84 RRab stars in the *GALEX* variable catalogs of Welsh et al. (2005) and Wheatley et al. (2008). We also classify 6  $\delta$  Scuti stars, 5 RRc stars and 18 RRab stars among the 55 variable *GALEX* sources identified as “stars” or RR Lyrae stars in the catalog of Gezari et al. (2013). We provide ephemerides and light curves for the 26 variables that were not previously known.

*Subject headings:* stars: RR Lyrae. stars:  $\delta$  Scuti, stars: variable. stars: red horizontal branch.

## 1. INTRODUCTION

The *Galaxy Evolution Explorer* (*GALEX*) (Martin et al. 2005) has imaged the whole sky in the *FUV* ( $\lambda\lambda$  1350 – 1750 Å) and *NUV* ( $\lambda\lambda$  1750 – 2750 Å) wavebands, opening the door to studying variable stars in the ultraviolet. One of the most important classes of variable stars are RR Lyraes, evolved horizontal branch stars that have intrinsic luminosities that correlate with pulsation amplitude and period.  $\delta$  Scuti stars (DSCT<sup>2</sup>) are a different class of pulsators with colors and pulsation periods comparable to RR Lyraes; they are discussed in the appendix (Sec. A). Importantly, the ultraviolet (*UV*) amplitudes of RR Lyrae stars are much larger in *GALEX* wavebands than in optical wavebands (Wheatley et al. 2003). What remains unexplored are complete samples of *UV* variables.

Interestingly, detailed observations of several bright RR Lyrae stars show that their *UV*–optical colors correlate with metallicity. Wheatley et al. (2012) fit model light-curves to the *FUV* and *NUV* photometry of six well-observed bright RR Lyrae stars. They find that the *FUV* and *NUV* light-curves, which primarily reflect temperature changes during the pulsation cycle, also depend on metallicity. We also find that  $(NUV - V)$  depends on metallicity.

To date, candidate variable *GALEX* sources have been cataloged by Welsh (2005) (Catalog 1) and by Wheatley et al. (2008) (Catalog 2). During the course of this work, a third catalog of over a thousand variable *GALEX* sources was published by Gezari et al. (2013); this cat-

alog exclusively uses *NUV* magnitudes. Few of these *UV* variables have optical identifications. Only 25% of the 84 sources in Catalog 1 and less than a third of the 410 sources in Catalog 2 are matched to optical objects of known type. Most of the *UV* variables with optical identifications are extragalactic objects. Less than 10% of the *UV* variables in the catalog of Gezari et al. (2013) have identifications with known types of stars.

The goal of this paper is to identify all of the Galactic stars in the *GALEX* variable catalogs in a complete and systematic way, with a particular focus on RR Lyrae variables. We investigate the  $(NUV - V)_0$  color index as a possible diagnostic for identifying variable types: in Sec. 4.5 and Appendix B, we address the problem of distinguishing between type c RR Lyrae stars and contact binaries (Kinman & Brown 2008). We base our analysis on *NUV* magnitudes, because *NUV* magnitudes are more accurate than *FUV* magnitudes and are available for a larger number of objects. The use of the  $(FUV - NUV)$  color could provide additional constraint (see for example, Smith et al. 2014) but would limit the sample.

Our approach is to use the VizieR search tool and the JAAVS variable star catalog (VSX, Watson 2006) to identify known variables, such as those identified by Drake et al. (2012) in the Catalina Surveys, by Palaversa et al. (2013) in the LINEAR Survey, and by Abbas et al. (2014) in their search of the combined SDSS, Pan-STARRS1 and Catalina Surveys<sup>3</sup>. We look at every object in Catalog 1 and in Catalog 2, and the subset of objects identified as “stars” in the larger Gezari catalog. If we are unable to classify an object with the variable star catalogs, we then use data from the Catalina Survey Data Release 2 (Drake et al. 2009) to measure the ob-

<sup>1</sup> NOAO is operated by AURA, Inc. under cooperative agreement with the National Science Foundation.

<sup>2</sup> These pulsating variables (spectral types A0 to F5) have *V* amplitudes in the range 0.03 to 0.90 mag.; those with *V* amplitudes greater than 0.20 are often called High Amplitude  $\delta$  Scuti stars.

<sup>3</sup> The Abbas et al. Catalog was published only shortly before this paper was completed and so it has only been possible to make limited use of it.

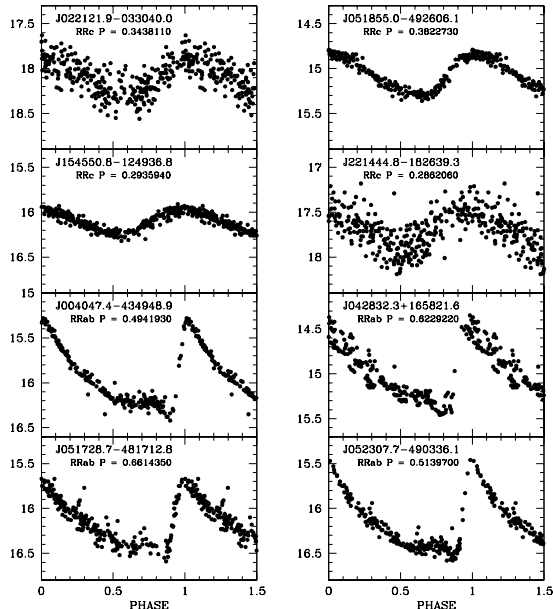


FIG. 1.—  $V$ -magnitude light curves for 4 newly identified RRc and 4 newly identified R Rab variables presented in Table 2.

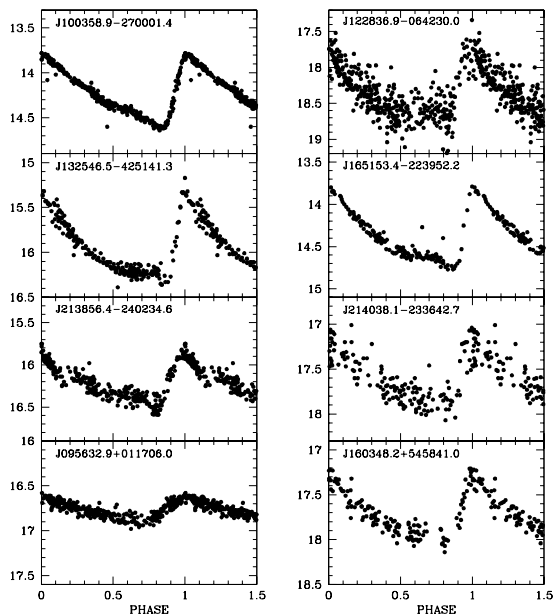


FIG. 2.—  $V$ -magnitude light curves for 8 new identified R Rab variables presented in Table 2.

ject's mean  $V$  magnitude and, if possible, its variability. Period-finding with the Catalina Survey data (e.g. using the NASA Exoplanet Archive Periodogram Service) becomes difficult for objects with  $V > 17$  and for objects with  $V$  amplitudes  $\lesssim 0.2$  magnitudes; consequently, the types we assign to such variables are less certain. We also review the 38 objects previously identified as RR Lyrae stars in the Gezari catalog.

This paper presents the RR Lyrae and  $\delta$  Scuti stars that we identify, and describes how *GALEX* magnitudes can assist in their identification. The  $(NUV - V)_0$  color is particularly sensitive for detecting the temperature changes that come from pulsations, and for detecting the onset of this instability as a function of parameters such

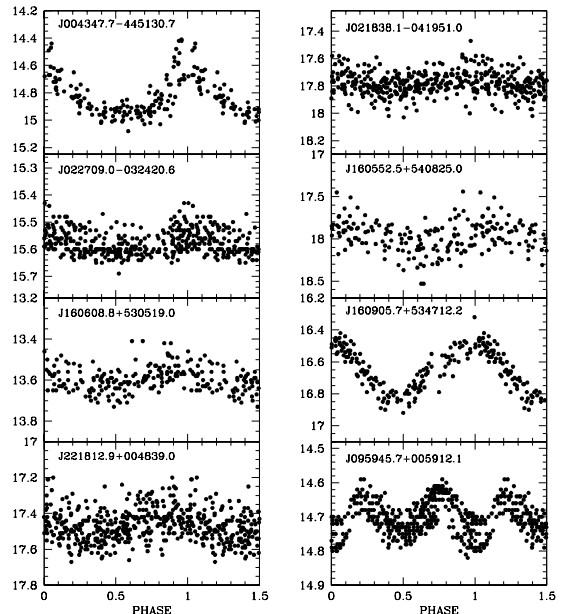


FIG. 3.—  $V$ -magnitude light curves for 7 newly identified  $\delta$  Scuti stars and one EW variable presented in Table 2. The periods of the lowest amplitude  $\delta$  Scuti stars are quite uncertain.

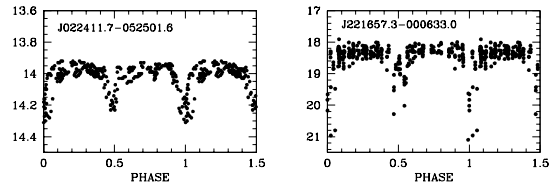


FIG. 4.—  $V$ -magnitude light curves for 2 newly identified Algol (EA) variables presented in Table 2. The period of J221657.3-000633.0 is uncertain.

as  $T_{\text{eff}}$ . The identification of other types of stars and variables from the *GALEX* variability catalogs will be discussed elsewhere.

## 2. THE IDENTIFICATION OF RR LYRAE AND $\delta$ Scuti STARS IN THE FIRST TWO *GALEX* VARIABILITY CATALOGS.

Table 1 presents 110 RR Lyrae and  $\delta$  Scuti stars that we identify from the first two catalogs of *GALEX* variables; these stars constitute 22% of all the sources in these catalogs. Our list comprises 8  $\delta$  Scuti stars, 17 RRc stars, 1 RRd star and 84 R Rab stars. References to the sources of the *GALEX* magnitudes and the optical data are given in columns 4 and 10 respectively. The  $(NUV - V)_0$  colors given in col. 8 refer to mean magnitudes<sup>4</sup> and their largest source of uncertainty lies in the estimation of the mean  $NUV$  from the available data; this uncertainty increases with the  $NUV$  amplitude and is therefore largest for the R Rab variables. We assumed the galactic extinction  $A(NUV) = 8.90E(B - V)$  (Rey et al. 2007). The  $E(B - V)$  were taken from the MAST archive of *GALEX* objects. Only 6 stars have  $E(B - V) > 0.100$  so the uncertainty in the correction for extinc-

<sup>4</sup> The mean  $NUV$  magnitude is the mean of the maximum and minimum values. The mean  $V$  magnitude is the arithmetic mean of all the observations given by the Catalina DataRelease 2. For brighter variables not in this survey, the mean was estimated from the maximum and minimum magnitudes using the formula given in the appendix of Preston et al. (1991).

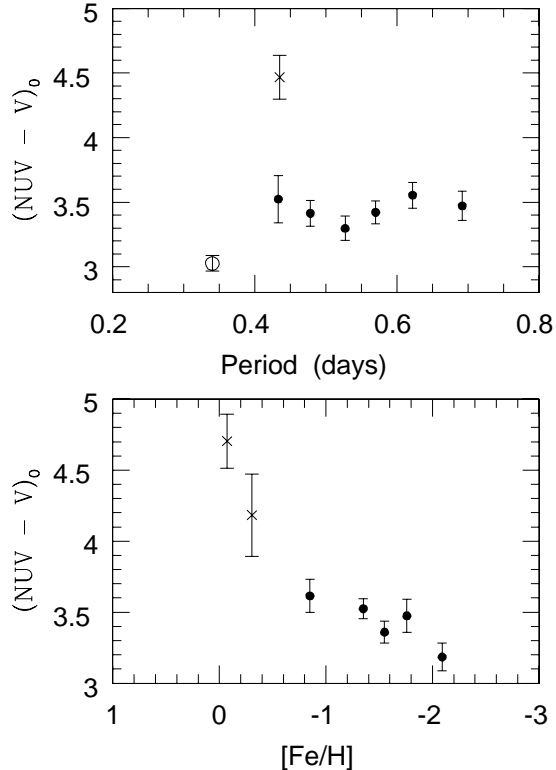


FIG. 5.— Distribution of known RR Lyrae stars from Dambis et al. (2013) in plots of the de-reddened  $(NUV - V)_0$  color versus period (upper panel) and versus  $[Fe/H]$  (lower panel). The filled circles, crosses, and open circles denote halo RRab, disk RRab, and RRC variables, respectively. There are significant differences in  $(NUV - V)_0$  between the disk RRab stars ( $[Fe/H] \geq -0.40$ ), the halo RRab stars ( $[Fe/H] \leq -0.80$ ), and the RRC stars.

tion (Peek & Schiminovich, 2013) is probably significant only for these stars. The periods given in column 9 are those taken from the literature in the case of previously known variables; otherwise, the periods were determined by us.

We discover 2 new  $\delta$  Scuti stars, 3 RRC stars and 10 RRab stars among the 110 variable stars. We present the ephemerides of the new variables in Table 2, and plot their light curves in Figures 1, 2, 3 & 4. One of these RRC and one of these RRab were later found in the catalog of Drake et al. (2014) but with differing periods; these differences are discussed in Sec. 4.6.

We investigate trends between  $(NUV - V)_0$  color and stellar properties by studying a well-defined sample of known RR Lyrae stars. We begin by calculating  $(NUV - V)_0$  for 150 nearby RR Lyrae stars using the recent compilation by Dambis et al. (2013), a sample for which we could easily obtain the necessary data. For this sample, we plot  $(NUV - V)_0$  against period for RRC and for *halo* and *disk* RRab (Fig 5, upper panel), and against  $[Fe/H]$  (Fig 5, lower panel).

There is a significant difference in  $(NUV - V)_0$  between the RRC and RRab that reflects the average temperature difference between the two types. There is also a significant difference in  $(NUV - V)_0$  between the *disk* and *halo* RRab that reflects the metallicity difference between the two types as expected from Wheatley et al. (2012).

We also investigate trends between the  $(NUV - V)_0$  color and stellar properties for a sample of known high-

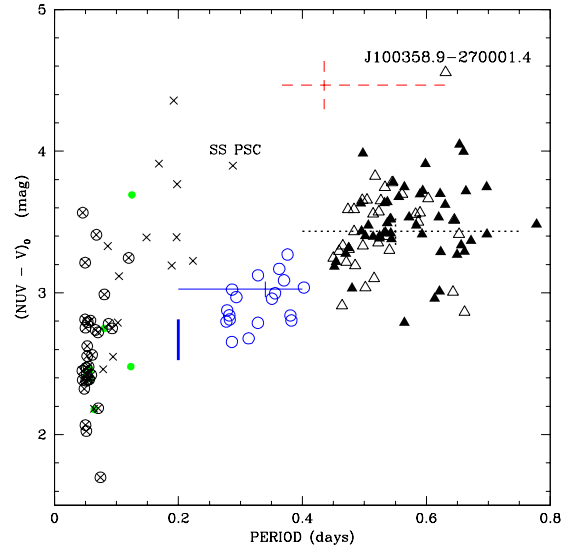


FIG. 6.— De-reddened  $(NUV - V)_0$  color versus pulsation period for our program stars from Table 1. The stars are plotted as: high-amplitude  $\delta$  Scuti stars (green solid circles), RRC (blue open circles), RRab from Catalog 1 (black open triangles) and RRab from Catalog 2 (black filled triangles). The blue (solid), black (dotted) and red (dashed) horizontal lines show mean values of  $(NUV - V)_0$  for known RRC, halo RRab, and disk RRab variables, respectively. Two samples of known high-amplitude  $\delta$  Scuti stars variables are plotted with black x's (McNamara 1997) and encircled black x's (Suveges et al. 2012). The heavy blue vertical line shows the range of  $(NUV - V)_0$  for blue horizontal branch stars at the blue edge of the instability gap (Kinman et al. 2007).

amplitude  $\delta$  Scuti stars (HADS) taken from McNamara (1997) and  $\delta$  Scuti of lower amplitude taken from Suveges et al. (2012). The results are shown in the plot of  $(NUV - V)_0$  vs. Period given in Fig. 6. The blue open circles, black open triangles and black filled triangles are respectively the RRC (both Catalogs), RRab from Catalog 1 and RRab from Catalog 2 in Table 1. The horizontal solid blue, dotted black and dashed red lines show the mean values of  $(NUV - V)_0$  for the RRC, halo RRab, and disk RRab respectively; their associated vertical lines show the *r.m.s.* standard errors of these means. There is good agreement between these mean values and the  $(NUV - V)_0$  of our program stars. The observed increase in this color with increasing period is nicely matched to the  $(NUV - V)_0$  location of the blue edge of the instability gap (Kinman et al. 2007), shown by the heavy blue vertical line at a period of 0.2 days in Fig. 6.

We discover three new RRab of particular interest. J100358.9-270001.4 has the largest  $(NUV - V)_0$  color and is the only object to lie in the color domain of the disk RR Lyrae stars. Yet at a heliocentric distance of roughly 5 kpc, it must be about 2 kpc above the galactic plane. Its proper motion of  $8 \pm 2$  mas  $y^{-1}$  (Girard et al., 2011) corresponds to a velocity of  $200 \pm 50$  km  $s^{-1}$ . This velocity and its relatively long pulsation period (0.6311 days) suggest that J100358.9-270001.4 is not a disk star, but a halo star. Spectroscopic radial velocity and metallicity measurements are needed to establish its origin. The two RRab stars with the smallest  $(NUV - V)_0$  colors are J165153.4-223952.2 and J214038.1-233642.7. J165153.4-223952.2 has the largest  $E(B - V) = 0.419$  and therefore the most uncertain extinction correction of the sample,

TABLE 1  
IDENTIFICATIONS OF  $\delta$  SCUTI (DCST) AND RR LYRAE STARS IN CATALOGS 1 AND 2. [AVAILABLE IN FULL IN THE ONLINE JOURNAL]

| Star <sup>a</sup>  | $NUV_{max}$ <sup>b</sup> | $NUV_{amp}$ <sup>c</sup> | Ref <sup>d</sup> | $E(B - V)$ | $V_{max}$ <sup>e</sup> | $V_{amp}$ <sup>f</sup> | $(NUV - V)_0$ <sup>g</sup> | Period <sup>h</sup> | Refs <sup>i</sup> | Notes        |
|--------------------|--------------------------|--------------------------|------------------|------------|------------------------|------------------------|----------------------------|---------------------|-------------------|--------------|
| DCST:              |                          |                          |                  |            |                        |                        |                            |                     |                   |              |
| J004347.9+421654.9 | 13.02                    | 0.63                     | 1,2              | 0.084      | 09.19                  | 0.27                   | 3.692                      | 0.1249078           | 13                | <b>1</b>     |
| J004347.7-445130.7 | 16.78                    | 0.84                     | 2                | 0.009      | 14.45                  | 0.50                   | 2.457                      | 0.0574790           | 20                | <b>2</b>     |
| J033715.2-283238.1 | 15.51                    | 0.94                     | 2                | 0.011      | 13.20                  | 0.65                   | 2.397                      | 0.0561380           | 11                |              |
| J104647.6+591445.5 | 19.86                    | 0.93                     | 2                | 0.008      | 17.40                  | 0.80                   | 2.480                      | 0.1231520           | 20                | <b>3</b>     |
| J133757.1+401610.8 | 20.00                    | 0.91                     | 1                | 0.006      | 18.00                  | 0.50                   | 2.177                      | 0.0641760           | 16                |              |
| J160608.8+530519.0 | 18.76                    | 1.53                     | 2                | 0.014      | 13.53                  | 0.55                   | 5.647                      | 0.1027590           | 20                | <b>2</b>     |
| J164106.8+404225.2 | 15.70                    | 0.87                     | 2                | 0.008      | 13.40                  | 0.55                   | 2.419                      | 0.0512960           | 13                | <b>4</b>     |
| J171250.9+582748.6 | 18.51                    | 0.63                     | 2                | 0.044      | 15.70                  | 0.30                   | 2.749                      | 0.0803930           | 16,7              | <b>5</b>     |
| RRc:               |                          |                          |                  |            |                        |                        |                            |                     |                   |              |
| J033546.0-290209.8 | 16.09                    | 0.90                     | 2                | 0.008      | 13.45                  | 0.50                   | 2.797                      | 0.2773379           | 18                |              |
| J051855.0-492606.1 | 17.59                    | 0.84                     | 2                | 0.026      | 14.85                  | 0.45                   | 2.806                      | 0.3822732           | 20                | <b>2</b>     |
| J103720.9+591653.8 | 18.31                    | 0.62                     | 2                | 0.008      | 15.70                  | 0.40                   | 2.679                      | 0.3132750           | 10,21,22          |              |
| J103759.4+581213.5 | 19.67                    | 1.03                     | 2                | 0.008      | 16.90                  | 0.40                   | 3.038                      | 0.4023800           | 21                | <b>2</b>     |
| J105044.4+045115.9 | 19.51                    | 0.97                     | 2                | 0.027      | 16.80                  | 0.45                   | 2.813                      | 0.2827820           | 16,19,22          |              |
| J143823.9+635329.9 | 19.23                    | 0.76                     | 2                | 0.016      | 16.34                  | 0.36                   | 2.998                      | 0.3559790           | 10,21             |              |
| J144033.3-781914.6 | 17.09                    | 0.79                     | 2                | 0.108      | 13.80                  | 0.70                   | 2.789                      | 0.3281820           | 13                | <b>6</b>     |
| J154550.8-124936.8 | 19.51                    | 0.62                     | 2                | 0.146      | 15.96                  | 0.28                   | 2.970                      | 0.2935940           | 20,22             | <b>2, 45</b> |
| J155800.6+535233.6 | 18.06                    | 0.87                     | 2                | 0.012      | 15.12                  | 0.36                   | 3.124                      | 0.3284030           | 16,10,21,22       |              |
| J160759.9+535209.9 | 19.20                    | 0.90                     | 2                | 0.012      | 16.52                  | 0.44                   | 2.841                      | 0.3806390           | 12,22             |              |
| J171008.9+585112.9 | 20.06                    | 0.92                     | 2                | 0.031      | 17.25                  | 0.50                   | 2.842                      | 0.2821010           | 16,21,22          |              |
| J203922.4-010346.0 | 16.88                    | 0.81                     | 2                | 0.084      | 13.57                  | 0.40                   | 3.089                      | 0.3703490           | 14,7,22           | <b>7</b>     |
| J204024.3-010950.0 | 19.06                    | 0.72                     | 2                | 0.079      | 15.68                  | 0.34                   | 3.170                      | 0.3626603           | 14,7,21           | <b>8</b>     |
| J204042.8-003717.3 | 20.28                    | 0.72                     | 2                | 0.159      | 17.12                  | 0.40                   | 3.023                      | 0.2865740           | 14,21             |              |
| J221444.8-182639.3 | 20.00                    | 0.96                     | 2                | 0.026      | 17.40                  | 0.55                   | 2.654                      | 0.2862060           | 20                | <b>2</b>     |
| J223601.0+134711.5 | 19.16                    | 0.91                     | 2                | 0.068      | 15.80                  | 0.40                   | 3.271                      | 0.3760710           | 16,7,22           | <b>9</b>     |
| J224029.0+120056.3 | 17.56                    | 0.85                     | 2                | 0.050      | 14.60                  | 0.50                   | 2.877                      | 0.2786230           | 16,7,21,22        | <b>10</b>    |
| RRd:               |                          |                          |                  |            |                        |                        |                            |                     |                   |              |
| J130204.5+463533.7 | 18.01                    | 1.45                     | 1                | 0.014      | 15.45                  | 0.60                   | 2.959                      | 0.3509191           | 12                | <b>11</b>    |
| RRab:              |                          |                          |                  |            |                        |                        |                            |                     |                   |              |
| J001611.6-392721.5 | 16.16                    | 2.02                     | 2                | 0.015      | 13.50                  | 1.00                   | 3.420                      | 0.5316009           | 11                |              |
| J003043.0-422747.7 | 17.25                    | 1.48                     | 2                | 0.007      | 14.00                  | 0.90                   | 3.747                      | 0.6973440           | 9                 |              |
| J004047.4-434948.9 | 18.20                    | 1.95                     | 2                | 0.016      | 15.30                  | 0.95                   | 3.633                      | 0.4941930           | 20                | <b>2</b>     |
| J004548.2-435509.1 | 16.00                    | 1.38                     | 1                | 0.001      | 13.00                  | 0.70                   | 3.565                      | 0.5898310           | 11                |              |
| J011010.9-452431.3 | 18.84                    | 1.85                     | 2                | 0.009      | 15.90                  | 0.85                   | 3.697                      | 0.5897626           | 13                | <b>12</b>    |
| J011805.2-751126.1 | 18.61                    | 1.41                     | 2                | 0.055      | 15.60                  | 1.20                   | 3.032                      | 0.480               | 13                | <b>13</b>    |
| J013642.0-062743.1 | 19.70                    | 0.63                     | 2                | 0.028      | 16.35                  | 0.25                   | 3.483                      | 0.7775660           | 16,7,22           | <b>14</b>    |
| J022521.8-050017.4 | 19.42                    | 1.57                     | 2                | 0.027      | 16.90                  | 0.80                   | 3.012                      | 0.6212419           | 3,21              |              |
| J033500.4-272854.8 | 16.98                    | 1.63                     | 2                | 0.009      | 14.20                  | 0.80                   | 3.415                      | 0.6975764           | 18                |              |
| J042832.3+165821.6 | 19.30                    | 1.64                     | 2                | 0.377      | 14.42                  | 1.00                   | 3.288                      | 0.6229220           | 20,7              | <b>2,15</b>  |
| J051728.7-481712.8 | 18.60                    | 1.42                     | 2                | 0.027      | 15.70                  | 0.80                   | 3.291                      | 0.6614350           | 20                | <b>2</b>     |
| J052307.7-490336.1 | 18.17                    | 2.13                     | 2                | 0.030      | 15.47                  | 1.10                   | 3.397                      | 0.5139700           | 20                | <b>2</b>     |
| J081226.4+033320.5 | 18.95                    | 1.95                     | 2                | 0.023      | 16.08                  | 0.72                   | 3.677                      | 0.5555151           | 6,7               | <b>16</b>    |
| J093026.0+071221.6 | 15.83                    | 0.97                     | 1                | 0.058      | 12.08                  | 0.79                   | 3.666                      | 0.6028494           | 13                | <b>17</b>    |
| J100133.2+014328.5 | 17.21                    | 1.98                     | 2                | 0.019      | 14.40                  | 1.00                   | 3.521                      | 0.5423741           | 3,10,19,21        |              |
| J100358.9-270001.4 | 18.26                    | 1.43                     | 1                | 0.079      | 13.78                  | 0.84                   | 4.556                      | 0.6311440           | 20                | <b>2</b>     |
| J102002.7+611538.9 | 16.71                    | 1.62                     | 1                | 0.007      | 14.34                  | 0.81                   | 3.005                      | 0.6428627           | 5,3,10,21         |              |
| J102641.8+572858.7 | 18.78                    | 1.84                     | 2                | 0.011      | 15.80                  | 0.85                   | 3.719                      | 0.6636605           | 10,21             |              |
| J103538.2+581549.1 | 15.53                    | 1.92                     | 2                | 0.008      | 12.87                  | 1.02                   | 3.384                      | 0.5242549           | 13,7              | <b>18</b>    |
| J104707.6+053349.2 | 17.78                    | 2.25                     | 2                | 0.024      | 15.00                  | 1.00                   | 3.642                      | 0.5369295           | 10,19,21          |              |
| J104803.1+554209.9 | 18.32                    | 2.14                     | 2                | 0.008      | 15.70                  | 1.05                   | 3.476                      | 0.5065280           | 10,21             |              |
| J104844.2+581538.6 | 18.47                    | 2.49                     | 2                | 0.011      | 16.10                  | 1.30                   | 3.317                      | 0.4748198           | 3,21              |              |
| J105130.9+043801.7 | 17.74                    | 2.03                     | 2                | 0.033      | 15.00                  | 1.00                   | 3.403                      | 0.5243170           | 16,10,19,21       |              |
| J105513.8+564747.7 | 17.09                    | 2.24                     | 2                | 0.007      | 14.65                  | 0.75                   | 3.519                      | 0.5417451           | 16,10             |              |
| J105622.3+570522.1 | 17.09                    | 2.27                     | 2                | 0.009      | 14.70                  | 0.90                   | 3.402                      | 0.5016290           | 3,10,21           |              |
| J105926.1-005927.9 | 19.53                    | 2.09                     | 1                | 0.042      | 16.72                  | 1.43                   | 3.246                      | 0.4499016           | 13,3,42           | <b>19</b>    |
| J111147.3+510549.4 | 18.12                    | 1.50                     | 1                | 0.014      | 15.10                  | 0.85                   | 3.514                      | 0.6449104           | 3                 |              |
| J112334.9+474014.6 | 19.45                    | 1.07                     | 1                | 0.014      | 16.18                  | 1.10                   | 3.353                      | 0.5224715           | 3,10,21           |              |
| J113340.3+502328.0 | 16.71                    | 2.93                     | 1                | 0.014      | 14.70                  | 1.10                   | 3.333                      | 0.4976910           | 13,21             | <b>20</b>    |

Truncated for display

REFERENCES. — (1) Welsh+(2005)(The *GALEX* Ultraviolet Variability Catalog); (2) Wheatley+(2008)(The Second *GALEX* Ultraviolet Variability Catalog); (3) Drake+(2013); (4) Keller+(2008); (5) Kinemuchi+(2006); (6) Kraus+(2007); (7) Li+(2011); (8) Miceli+(2008); (9) Norton+(2007); (10) Palaversa+(2013); (11) Pojmanski(2002)(ASAS Catalogue); (12) Poleski(2013); (13) Samus+(2012)(Gen. Cat. Variable Stars); (14) Sesar+(2010); (15) Vivas+(2004)(QUEST Survey); (16) Watson+(2006)(AAVSO VSX Catalog); (17) Wils+(2006); (18) Wils(2010)(Data in VSX Catalog); (19) Zinn+(2014)(Extension of QUEST Survey); (20) This Paper (New Identification). (21) Abbas+ (2014); (22) Drake+ (2014).

NOTE. — (1) CC And. (2) New identification. Ephemeris in Table 2. (3) New Identification. Type and period uncertain. (4) v1209 Her (SX Phe type). (5) Sp Type A (7) (6) v344 Aps. (7) Sp Type A (7) (8) Sp Type F (7) (9) Sp Type A (7) (10) Sp Typ A (7) (11) Period is first overtone. (12) UU Phe. (13) BG Tuc, B magnitude. (14) Sp Typ A (7) (15) Sp Typ F (7) (16) Sp Typ F (7) (17) WW Leo. (18) v341 Uma; Sp Type A (7). (19) IX Leo. (20) CZ Uma.

<sup>a</sup> *GALEX* identification of source.

<sup>b</sup> *NUV* magnitude at maximum.

<sup>c</sup> Amplitude of *NUV* magnitude.

<sup>d</sup> Reference for *GALEX* source.

<sup>e</sup> *V* magnitude at maximum.

<sup>f</sup> Amplitude of *V* magnitude.

<sup>g</sup> Difference between mean *NUV* and *V* magnitudes corrected for galactic extinction.

<sup>h</sup> Period in days.

<sup>i</sup> References for optical data.

TABLE 2  
POSITIONS, TYPES AND EPHEMERIDES OF NEW<sup>†</sup> VARIABLES.

| Star <sup>a</sup>               | R.A. <sup>b</sup><br>(2000) | Dec. <sup>c</sup><br>(2000) | Type <sup>d</sup> | HJD(max) <sup>e</sup><br>2450000.0+ | Period <sup>f</sup><br>(days) | $V_{max}$ <sup>g</sup><br>(mag.) | $V_{min}$ <sup>h</sup><br>(mag.) |
|---------------------------------|-----------------------------|-----------------------------|-------------------|-------------------------------------|-------------------------------|----------------------------------|----------------------------------|
| CATALOGS 1 and 2:               |                             |                             |                   |                                     |                               |                                  |                                  |
| J004347.7–445130.7              | 010.9488                    | –44.8586                    | DCST              | 3556.1599                           | 0.057479                      | 14.45                            | 14.95                            |
| J160608.8+530519.0              | 241.5371                    | +53.0890                    | DCST              | 3656.5589                           | 0.102759                      | 13.53                            | 13.64                            |
| J051855.0–492606.1              | 079.7293                    | –49.4349                    | RRc               | 3578.5038                           | 0.382273                      | 14.85                            | 15.30                            |
| J154550.8–124936.8 <sup>‡</sup> | 236.4618                    | –12.8269                    | RRc               | 3523.4753                           | 0.293594                      | 15.96                            | 16.24                            |
| J221444.8–182639.3              | 333.6870                    | –18.4444                    | RRc               | 3583.6795                           | 0.286206                      | 17.40                            | 17.95                            |
| J004047.4–434948.9              | 010.1981                    | –43.8301                    | RRab              | 3555.8138                           | 0.494193                      | 15.30                            | 16.25                            |
| J042832.3+165821.6              | 067.1349                    | +16.9726                    | RRab              | 3469.5764                           | 0.622922                      | 14.45                            | 15.45                            |
| J051728.7–481712.8              | 079.3700                    | –48.2869                    | RRab              | 3576.4696                           | 0.661435                      | 15.70                            | 16.50                            |
| J052307.7–490336.1              | 080.7823                    | –49.0599                    | RRab              | 3576.4712                           | 0.513970                      | 15.47                            | 16.57                            |
| J100358.9–270001.4              | 150.9955                    | –27.0002                    | RRab              | 3694.8098                           | 0.631144                      | 13.78                            | 14.62                            |
| J122836.9–064230.0 <sup>‡</sup> | 187.1540                    | –06.7085                    | RRab              | 3496.5066                           | 0.501648                      | 17.50                            | 18.60                            |
| J132546.5–425141.3              | 201.4437                    | –42.8615                    | RRab              | 3556.7107                           | 0.451759                      | 15.25                            | 16.25                            |
| J165153.4–223952.2              | 252.9728                    | –22.6644                    | RRab              | 3599.5306                           | 0.613432                      | 13.80                            | 14.75                            |
| J213856.4–240234.6              | 324.7351                    | –24.0430                    | RRab              | 3597.8294                           | 0.594016                      | 15.80                            | 16.55                            |
| J214038.1–233642.7              | 325.1592                    | –23.6118                    | RRab              | 3638.7051                           | 0.564344                      | 17.25                            | 17.90                            |
| Gezari et al. (2013):           |                             |                             |                   |                                     |                               |                                  |                                  |
| J022709.0–032420.6              | 036.7872                    | –03.4058                    | DCST              | 3648.7343                           | 0.1685980                     | 16.60                            | 16.69                            |
| J221812.8+004839.0              | 334.5535                    | +00.8106                    | DCST              | 3507.9368                           | 0.0413220                     | 17.35                            | 17.50                            |
| J160552.5+540825.0              | 241.4690                    | +54.1404                    | DCST              | 3880.8828                           | 0.0587400                     | 17.70                            | 18.10                            |
| J160905.7+534712.2 <sup>‡</sup> | 242.2740                    | +53.7866                    | DCST              | 3505.5268                           | 0.1697210                     | 16.50                            | 16.85                            |
| J021838.1–041951.0              | 034.6589                    | –04.3304                    | DCST              | 3627.8700                           | 0.0759360                     | 17.70                            | 17.80                            |
| J022121.9–033040.0 <sup>‡</sup> | 035.3413                    | –03.5109                    | RRc               | 3627.5444                           | 0.3438110                     | 17.90                            | 18.30                            |
| J095632.9+011706.0              | 149.1372                    | +01.2850                    | RRab              | 3464.1026                           | 0.7711330                     | 16.60                            | 16.69                            |
| J160348.2+545841.0              | 240.9508                    | +54.9780                    | RRab              | 3880.6148                           | 0.5418940                     | 17.25                            | 18.05                            |
| J095945.7+005912.1              | 149.9400                    | +00.9866                    | EW                | 3464.4354                           | 0.2874170                     | 14.62                            | 14.75                            |
| J221657.3–000633.0              | 334.2392                    | –00.1091                    | EA                | 3502.9800                           | 18.32325                      | 18.30                            | 20.:                             |
| J022411.7–052501.6 <sup>‡</sup> | 036.0485                    | –05.4172                    | EA                | 3627.8052                           | 0.8254050                     | 13.95                            | 14.3:                            |

<sup>†</sup> All stars in this table had not been identified as variables prior to 2014 May 29.

<sup>a</sup> *GALEX* identification of source.

<sup>b</sup> Right Ascension in decimal degrees.

<sup>c</sup> Declination in decimal degrees.

<sup>d</sup> Variable Type.

<sup>e</sup> Heliocentric Julian Date of Maximum.

<sup>f</sup> Period in days.

<sup>g</sup>  $V$  magnitude at maximum.

<sup>h</sup>  $V$  magnitude at minimum.

<sup>‡</sup> These stars were identified as variables by Drake et al. (2014).

TABLE 3  
DATA FOR THE VARIABLE STARS IDENTIFIED BY GEZARI ET AL. (2013) .

| (2000)   | R.A. <sup>a</sup><br>(2000) | Dec. <sup>b</sup><br>(2000) | $NUV_{amp}$ <sup>c</sup><br>(mag.) | LC <sup>d</sup> | $(NUV - V)_0$ <sup>e</sup><br>(mag.) | Period <sup>f</sup><br>(days) | $V^g$<br>(mag.) | $(B - V)$ <sup>h</sup><br>(mag.) | Type <sup>i</sup> | Type <sup>j</sup> | Type <sup>k</sup> | Notes |
|----------|-----------------------------|-----------------------------|------------------------------------|-----------------|--------------------------------------|-------------------------------|-----------------|----------------------------------|-------------------|-------------------|-------------------|-------|
| 212.2576 | +53.1997                    | 0.24                        | V                                  | 3.298           | ...                                  | 16.39                         | +0.52           | RR                               | RR                | ...               |                   |       |
| 36.7721  | -03.7063                    | 0.36                        | V                                  | 1.896           | ...                                  | 16.54                         | +0.26           | RR                               | RR                | ...               |                   |       |
| 36.7872  | -03.4058                    | 0.37                        | V                                  | 2.103           | 0.1685980                            | 15.51                         | +0.32           | RR                               | RR                | $\delta$ Scuti    | (1)(18)           |       |
| 36.4632  | -04.8917                    | 0.43                        | V                                  | 1.912           | ...                                  | 16.73                         | +0.19           | RR                               | RR                | ...               |                   |       |
| 334.5535 | +00.8106                    | 0.45                        | V                                  | 1.728           | 0.0413220                            | 17.30                         | +0.21           | RR                               | RR                | $\delta$ Scuti    | (1)               |       |
| 150.0513 | +01.0615                    | 0.46                        | V                                  | 3.361           | ...                                  | 17.19                         | +0.49           | RR                               | RR                | ...               |                   |       |
| 150.0909 | +01.2796                    | 0.49                        | V                                  | 4.477           | 0.3162890                            | 14.82                         | +0.61           | RR                               | RR                | EW                | (2)(22)           |       |
| 34.6594  | -04.3309                    | 0.51                        | V                                  | 2.280           | 0.0759360                            | 17.72                         | +0.26           | RR                               | RR                | $\delta$ Scuti    | (1)               |       |
| 332.9349 | -00.4230                    | 0.63                        | V                                  | 1.782           | ...                                  | 17.42                         | +0.50           | RR                               | RR                | ...               |                   |       |
| 149.1372 | +01.2850                    | 0.73                        | V                                  | 3.359           | 0.7711330                            | 16.69                         | +0.37           | RR                               | RR                | RRab              | (1)               |       |
| 149.6863 | +02.5218                    | 0.79                        | V                                  | 3.553           | 0.6468498                            | 17.61                         | +0.47           | RR                               | RR                | RRab              | (3)               |       |
| 241.4690 | +54.1404                    | 0.80                        |                                    | 2.376           | 0.0587400                            | 17.96                         | +0.32           | RR                               | RR                | $\delta$ Scuti    | (1)               |       |
| 242.2740 | +53.7866                    | 0.89                        |                                    | 3.882           | 0.1697210                            | 16.61                         | +0.54           | RR                               | RR                | $\delta$ Scuti    | (1)(23)           |       |
| 241.9999 | +53.8693                    | 0.95                        | V                                  | 2.619           | 0.3806406                            | 16.71                         | +0.20           | RR                               | RR                | RRab              | (4,5)             |       |
| 35.3413  | -03.5109                    | 0.95                        | V                                  | 2.820           | 0.3438094                            | 18.04                         | +0.29           | RR                               | RR                | RRc               | (1,7,22)          |       |
| 333.3199 | -00.5376                    | 0.95                        |                                    | 2.114           | 0.3365870                            | 16.66                         | -0.45           | RR                               | RR                | RRc               | (6,21,22)         |       |
| 333.5874 | +01.3271                    | 0.96                        |                                    | 4.347           | ...                                  | 17.22                         | +0.55           | RR                               | RR                | ...               |                   |       |
| 332.4833 | -00.6473                    | 0.99                        | V                                  | 2.290           | 0.3016423                            | 16.05                         | +0.22           | RR                               | RR                | RRc               | (8,9,21,22)       |       |
| 215.9569 | +52.6509                    | 1.00                        | V                                  | 0.961           | ...                                  | 20.30                         | +0.53           | RR                               | RR                | ...               |                   |       |
| 150.2291 | +01.3947                    | 1.00                        | V                                  | 2.651           | 0.3210413                            | 15.75                         | +0.36           | RR                               | RR                | RRc               | (2,21,22)         |       |
| 216.3439 | +52.7295                    | >1.04                       | F                                  | >3.263          | ...                                  | 19.42                         | +0.46           | RR                               | RR                | ...               |                   |       |
| 214.0191 | +52.4641                    | 1.11                        | V                                  | 3.532           | 0.5825432                            | 16.41                         | +0.51           | RR                               | RR                | RRab              | (2,3)             |       |
| 333.8419 | +00.5817                    | 1.18                        | V                                  | 0.960           | ...                                  | 20.07                         | +0.26           | RR                               | RR                | $\delta$ Scuti ?  | (10)              |       |
| 212.8810 | +53.5101                    | 1.29                        |                                    | 3.375           | 0.5807728                            | 16.54                         | +0.41           | RR                               | RR                | RRab              | (11,21,22)        |       |
| 150.5272 | +01.3757                    | 1.41                        | V                                  | 3.271           | 0.7289104                            | 16.28                         | +0.50           | RR                               | RR                | RRab              | (2,3,21)          |       |
| 332.8058 | -00.3874                    | 1.55                        | V                                  | 2.612           | 0.5807727                            | 16.98                         | +0.33           | RR                               | RR                | RRab              | (2,21)            |       |
| 242.8745 | +53.7296                    | 1.57                        | V                                  | 3.052           | 0.5838609                            | 16.07                         | +0.52           | RR                               | RR                | RRab              | (2,4,12,21)       |       |
| 334.4712 | -00.0933                    | 1.71                        | V                                  | 2.876           | 0.6556452                            | 13.93                         | +0.37           | RR                               | RR                | RRab              | (13)              |       |
| 241.8077 | +55.8589                    | 1.85                        |                                    | 3.286           | 0.5464062                            | 15.92                         | +0.18           | RR                               | RR                | RRab              | (2,3,4,21)        |       |
| 241.2133 | +54.1410                    | 1.89                        |                                    | 2.997           | 0.5161044                            | 16.55                         | +0.13           | RR                               | BHB               | RRab              | (2,3)             |       |
| 334.2392 | -0.1091                     | >1.91                       | F                                  | >2.754          | 18.32325                             | 18.20                         | +0.24           | RR                               | RR                | EA                | (1,14)            |       |
| 150.3887 | +01.7245                    | 1.93                        | V                                  | 3.047           | 0.5423790                            | 14.91                         | +0.26           | RR                               | RR                | RRab              | (2,3,4,21)        |       |
| 36.3486  | -05.5392                    | 2.07                        | V                                  | 2.832           | 0.5363961                            | 16.79                         | +0.46           | RR                               | RR                | RRab              | (3,20,21)         |       |
| 240.9508 | +54.9780                    | 2.11                        | V                                  | 3.465           | 0.5418940                            | 17.71                         | +0.24           | RR                               | RR                | RRab              | (1)               |       |
| 36.3409  | -05.0050                    | 2.30                        | V                                  | 2.888           | 0.6212305                            | 17.27                         | +0.46           | RR                               | RR                | RRab              | (3,21)            |       |
| 150.1707 | +01.3682                    | >2.70                       | V                                  | >3.115          | 0.4888790                            | 18.55                         | +0.16           | RR                               | BHB               | RRab              | (3)               |       |
| 332.9690 | 0.6330                      | 2.91                        | V                                  | 2.633           | 0.5053500                            | 16.73                         | +0.31           | RR                               | RR                | RRab              | (3,21)            |       |
| 333.0054 | -0.0571                     | 2.92                        | V                                  | 2.680           | 0.5030960                            | 17.42                         | +0.32           | QSO                              | RRab              | RRab              | (6)               |       |
| 36.0485  | -05.4172                    | 1.03                        | F                                  | 5.38            | 0.8254050                            | 13.94                         | 0.89            | ...                              | Star              | EA                | (1,15,24)         |       |
| 150.8023 | +00.9722                    | 1.00                        | F                                  | 3.74            | 0.6061280                            | 16.08                         | 0.55            | ...                              | Star              | RRab              | (3)(19)           |       |
| 333.0985 | +00.0828                    | 0.96                        | V                                  | 2.18            | 0.3505063                            | 15.85                         | 0.17            | ...                              | Star              | RRc               | (6,22)            |       |
| 149.9732 | +03.2086                    | 0.72                        | V                                  | 4.91            | 0.2738640                            | 15.12                         | 0.69            | ...                              | Star              | EA                | (2,22)            |       |
| 215.2242 | +54.4815                    | 0.61                        |                                    | 5.24            | 0.3586440                            | 13.92                         | 0.58            | ...                              | Star              | EW                | (16,22)           |       |
| 35.5465  | -03.1702                    | 0.57                        | V                                  | 4.63            | 0.4051308                            | 13.14                         | 0.60            | ...                              | Star              | EW                | (17,15,22)        |       |
| 149.9400 | +00.9866                    | 0.27                        | V                                  | 4.44            | 0.2874170                            | 14.63                         | 0.66            | ...                              | Star              | EW                | (1)               |       |

NOTE. — (1) New Identification (this paper). (2) Palaversa et al. (2013). (3) Drake et al. (2012). (4) Wheatley et al. (2008) Second *GALEX* catalogue of variables. (5) Drake et al. (2014) give type and period. Poleski (2014) gives same period. (6) Sesar et al. (2010). (7) Radial velocity  $-154 \pm 2$  km s<sup>-1</sup> (SDSS DR 9). (8) Sesar et al. (2012). (9) Radial velocity  $-213 \pm 1$  km s<sup>-1</sup> (SDSS DR 9). (10) New Identification. Possible HADS but period uncertain. (11) CL Boo. (12) Radial velocity  $-302 \pm 2$  km s<sup>-1</sup> (SDSS DR 9). (13) GG Aqr. (14) Faint object: Period and depth of minima uncertain. Drake et al. (2014) give Period of 2.23825 days. Radial velocity  $+29 \pm 5$  km s<sup>-1</sup> (SDSS DR 9). (15) X-ray source (Flesch, 2010) (16) KM Boo. (17) Pojmanski (2002). (18)  $(B - V) = 0.28$ ;  $[\text{Fe}/\text{H}] = -1.56$ ; Radial Velocity  $= -14 \pm 14$  (Brown et al., 2008). (19) Radial velocities  $+76 \pm 6$  &  $+159 \pm 3$  (SDSS DR 9). (20)  $[\text{C}/\text{Fe}] = +3.4$  (Christlieb et al., 2008). (21) Abbas et al. (2014). (22) Drake et al. (2014). (23) Drake et al. (2014) give type as EW and period of 0.339 days. See Sec. 4.6 for discussion. (24) Drake et al. (2014) give same type and period of 0.583 days. See Sec. 4.6 for discussion.

<sup>a</sup> Right Ascension in decimal degrees.

<sup>b</sup> Declination in decimal degrees.

<sup>c</sup> Amplitude of  $NUV$ .

<sup>d</sup> Light curve type: V = Stochastic; F = Flaring (Gezari et al., 2013).

<sup>e</sup> Difference between mean  $NUV$  and  $V$  magnitudes corrected for galactic extinction.

<sup>f</sup> Period in days.

<sup>g</sup> Mean  $V$  corrected for extinction.

<sup>h</sup> Mean  $(B - V)$  corrected for extinction.

<sup>i</sup> Variable type from color (Gezari et al., 2013).

<sup>j</sup> Variable type (Gezari et al., 2013); RR = RR Lyrae, BHB = blue HB star.

<sup>k</sup> Variable type (This paper). EA are Algol-type eclipsing systems. EW are W Ursa Majoris-type eclipsing systems.

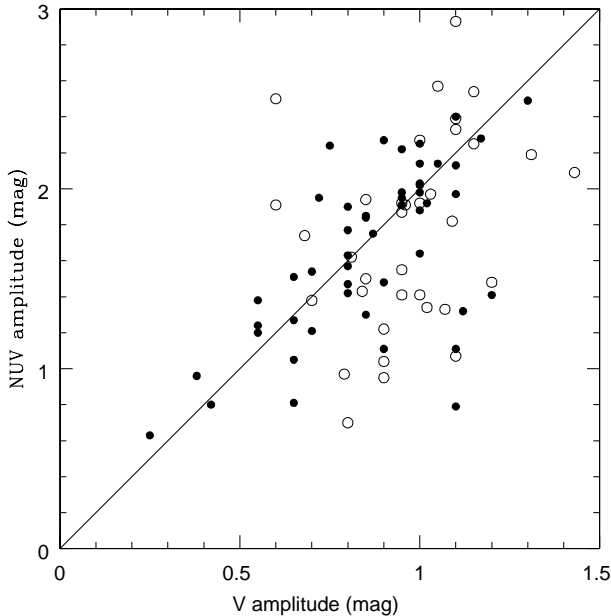


FIG. 7.— The relation between the *NUV* amplitude and the *V* amplitude for 84 type RRab variables. The line corresponds to the case where the *NUV* amplitude is twice the *V* amplitude. The variables from Catalog 1 (open circles) lie preferentially below the line while those from Catalog 2 (filled circles) are more equally above and below the line.

while J214038.1-233642.7 has an unusually low *V* amplitude for its period and is possibly multiperiodic.

The high amplitude  $\delta$  Scuti stars in Table 1 are shown by green filled circles in Fig. 6 and lie within the domain of the known  $\delta$  Scuti stars which show a wide range in  $(NUV - V)_0$ . We note that the star SS Psc, which has a conflicting RRc classification in the GCVS and a  $\delta$  Scuti star classification by McNamara (1997), is clearly in the  $\delta$  Scuti star domain.

### 3. THE IDENTIFICATION OF RR LYRAE AND $\delta$ Scuti STARS IN THE GEZARI ET AL. (2013) CATALOG.

In Table 3 we present updated classifications and period measurements for 28 of the 38 RR Lyrae stars identified by Gezari et al. (2013). We find that 16 are RRab, 4 are RRc, 6 are  $\delta$  Scuti stars and 2 are eclipsing systems. The main reason that we could not obtain acceptable light-curves for the remaining objects was because their visual amplitudes were comparable to the observational errors of their magnitudes. A fuller discussion is given in Sec. 4.6.

Interestingly, Gezari et al. (2013) provide a “light curve type” (LC) which is either Stochastic (V) or Flaring (F) (col. 4, Table 3). We would expect that RR Lyrae and  $\delta$  Scuti stars to have “Stochastic” light curves, but two of the variables that Gezari et al. type as RR Lyrae have “Flaring” light curves in *NUV*.

Another 17 variables in the Gezari catalog are identified simply as “Stars.” We are able to make detailed classifications for 7 of these objects, listed at the end of Table 3. We identify 1 RRab, 1 RRc and 5 eclipsing systems. Five of the “Stars” from the Gezari catalog have “Flaring” light curves: 1 is an RRab, 2 are eclipsing systems and 2 are of unknown type.

We provide ephemerides for the eleven newly identified variables from the Gezari catalog in Table 2.

## 4. DISCUSSION

We investigate the stellar properties of our sample of *UV*-selected variables. We compare *NUV* pulsation amplitudes with optical *V* amplitudes, with the distribution of pulsation periods, and with the distribution of non-variable stars. We explore the completeness of the *UV*-selected sample, the problem of distinguishing between contact binaries and pulsating stars and finally with a comparison of periods obtained in this paper with those independently obtained in a contemporaneous compilation by Drake et al. (2014).

### 4.1. The relation between the *NUV* and *V* amplitudes.

We begin by exploring the distribution of *NUV* and *V* pulsation amplitudes of the *GALEX* variables. For context, consider the five RRab variables with well-observed *NUV* light curves from Wheatley et al. (2012). The mean of the ratio of the *NUV* amplitudes to the corresponding *V* amplitudes (taken from the literature) for these five RRab stars is  $2.15 \pm 0.18$ . The  $[\text{Fe}/\text{H}]$  of these stars range from  $-1.5$  to  $-1.7$  (mean  $-1.64$ ), which means they are typical halo RR Lyrae stars.

In Figure 7 we plot the *NUV* amplitude *vs.* the *V* amplitude for the 84 RRab variables in Table 1. The variables from Catalog 1 are plotted as open circles and those from Catalog 2 by filled circles. The line represents the case where the *NUV* amplitude is twice that of the *V* amplitude. In this figure, 11 of the RR Lyrae from Catalog 1 lie above the line and 24 below; 26 of the variables from Catalog 2 lie above the line and 23 below. The Catalog 1 variables lie preferentially below the line (5% level of significance) while those from Catalog 2 are more equally spaced. Thus the *NUV* amplitudes for the RRab derived from Catalog 1 are on average lower than those from Catalog 2; the latter are generally derived from more observations and approximate more closely to the true amplitudes. The scatter in Fig. 7 is large so that the correlation between the *NUV* and *V* amplitudes is not strong. It is clear, however, that on average the RRab *NUV* amplitudes are twice as large as their *V* amplitudes.

### 4.2. The log period-amplitude relation for *NUV* and *V* amplitudes.

Next we explore the period-amplitude relation of the variables. In Figure 8 we plot the distribution of  $\log(\text{period})$  versus *NUV* amplitudes (left panel) and *V* amplitudes (right panel). For reference, the curve shows the relation for Oosterhoff Type I RRab variables observed in the globular cluster M3 (Cacciari et al. 2008). The curve refers to monopерiodic variables; curves with secondary periods such as RRd or those with Blazhko effect will have smaller amplitudes and lie below the line in this plot. In the right hand plot, the variables with periods shorter than 0.56 days ( $\log P \leq -0.25$ ) lie mainly below the curve; those with longer periods lie increasingly above the curve with increasing period. We suspect that our *V* amplitudes (derived by visual inspection from light-curves largely derived from Catalina Survey data (Drake et al., 2009) or in a few cases LINEAR Survey data (Sesar et al., 2013)) are systematically too small and that the admixture of higher amplitude variables with periods greater than 0.56 days comes from a

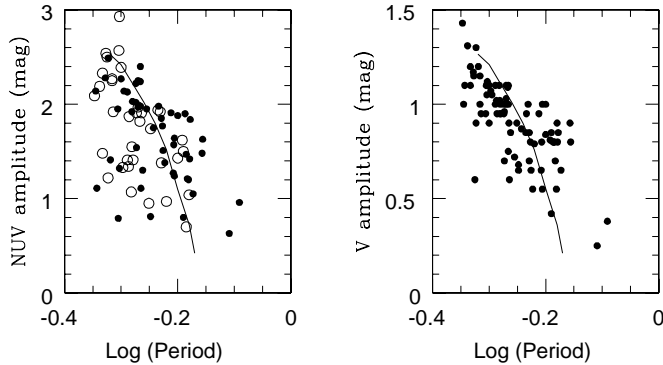


FIG. 8.— Amplitude *vs.* log period relation for the  $NUV$  amplitude (left panel) and  $V$  amplitude (right panel) for the 84 RRab variables from Catalog 1 (open circles) and Catalog 2 (solid circles). The curve is the relation found for the Oosterhoff type 1 variables in the globular cluster M3 given by Cacciari et al. (2008); the amplitude of the curve has been doubled for the  $NUV$  amplitudes in the left panel.

population of Oosterhoff type II variables. The errors in the amplitudes are too great for a clean separation of the two types. A similar interpretation holds for the  $NUV$  amplitudes in the left plot in Fig. 8 although the scatter is larger.

Two stars of interest are J013642.0-062743.1 and J171251.8+185452.4, which have periods 0.7775660 and 0.8111936 days, respectively, and amplitudes less than 0.4 mag. Schmidt (2002) has studied stars with periods between 0.60 and 1.0 days and explored the various types of variables in this range. He finds 6 RRab with periods greater than 0.75 days and only 4 with periods greater than 0.80 days. None of these stars have amplitudes less than 0.50 mag. A new survey by Abbas et al. (2014) finds  $\sim 20$  RRab with periods greater than 0.80 days. Most of these stars have  $V$  amplitudes between 0.4 and 0.6 magnitudes, and constitute about 0.03% of their total sample. Here, we find two RRab with smaller amplitudes in this period range, the aforementioned J013642.0-062743.1 and J171251.8+185452.4. These two RRab constitute  $\sim 2\%$  of our sample, suggesting that the use of *GALEX* magnitudes (where observed amplitudes are larger) facilitates the discovery of such low amplitude stars.

#### 4.3. The Red Horizontal Branch (RHB) stars.

In the plot of  $(NUV - V)_0$  against period, the hottest RR Lyrae stars (type RRc) are coterminous with the blue horizontal branch stars at the blue edge of the instability gap. The stars near this blue edge are nearly all metal-poor; thick disk blue horizontal branch stars are rare (Kinman et al. 2009).

We now consider the non-variable horizontal branch stars on the cool side of the instability gap: the red horizontal branch (RHB) stars. Fig. 9 plots  $(NUV - V)_0$  against effective temperature ( $T_{eff}$ ) for these stars. The sources for the data in this plot are given in the Appendix (Sec. C). We see that the hottest metal-poor RHB stars have  $(NUV - V)_0$  colors similar to the halo RR Lyrae stars. Indeed, we find that some of the hottest metal-poor RHB candidates are actually RR Lyrae stars.

For  $T_{eff}$  less than about 5200 K, most of these RHB stars are metal-rich ( $[Fe/H] > -0.8$ ) and have larger  $(NUV - V)_0$  than the metal-poor RHB, similar to the

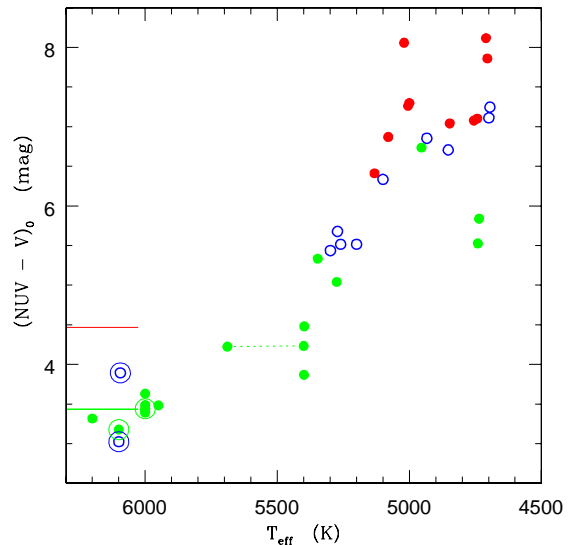


FIG. 9.—  $(NUV - V)_0$  color versus spectroscopic effective temperature  $T_{eff}$  for a selection of red horizontal branch (RHB) stars. Colors indicate metallicity:  $[Fe/H] > -0.80$  are shown by red filled circles,  $-0.8 > [Fe/H] > -1.70$  are blue open circles, and  $[Fe/H] < -1.70$  are green filled circles. The two measurements for HD 119516 are joined by a dotted line. Four stars are optical variables and are indicated by encircled symbols (bottom left). The red and green horizontal lines show the mean values of  $(NUV - V)_0$  for disk and halo RRab variables (as shown in Fig. 6). The data and notes on individual stars are presented in Table A3 in the Appendix.

trend seen in the RRab stars. We do not find any metal-rich RHB stars hotter than this limit. As we discuss in Appendix C, this is likely an observational selection effect; there are few constraints on hot metal-rich RHB stars at fainter magnitudes ( $V > 10.5$ ). We cannot rule out, however, that hot metal-rich RHB stars may be scarce in the field even though they are found in the metal-rich globular clusters like 47 Tuc.

The change in  $(NUV - V)_0$  color with effective temperature is much larger compared with the change in optical color indices. Stars like BD 18° 2757 and BPS CS 22875-029 have similar metallicity but differ in  $T_{eff}$  by  $\sim 1250$  K. Their difference in  $(B - V)_0$  and  $(J - K)_0$  are 0.32 and 0.15 mag, respectively, while their difference in  $(NUV - V)_0$  is over 2 mag. This makes the  $(NUV - V)_0$  color particularly sensitive for detecting the temperature changes that come from pulsations and, in particular, for detecting the onset of this instability as a function of other parameters (such as  $T_{eff}$ ).

#### 4.4. The Completeness of the Samples.

We explore the magnitude limits of our samples in Figure 10. Fig. 10(a) plots the distribution of the minimum  $V$  magnitudes for the 84 RRab variables in Table 1. There is a steep fall-off in the distribution at  $V \sim 17.5$ . Fig. 10(b) and Fig. 10(c) plot the distribution of the faintest observed  $NUV$  of the RRab in Catalogs 2 and 1, respectively. There is a steep fall-off at about  $(NUV) = 21.0$ . These two magnitude limits are consistent with the  $3.4 \leq (NUV - V) \leq 3.8$  mag RRab colors observed by Wheatley et al. (2012); most of the RRab in Table 1 are also in this range.

A  $V=17.5$  magnitude corresponds to a distance limit of about 25 kpc for our sample of RRab. Most of the stars in our sample are at a sufficiently high galactic latitude



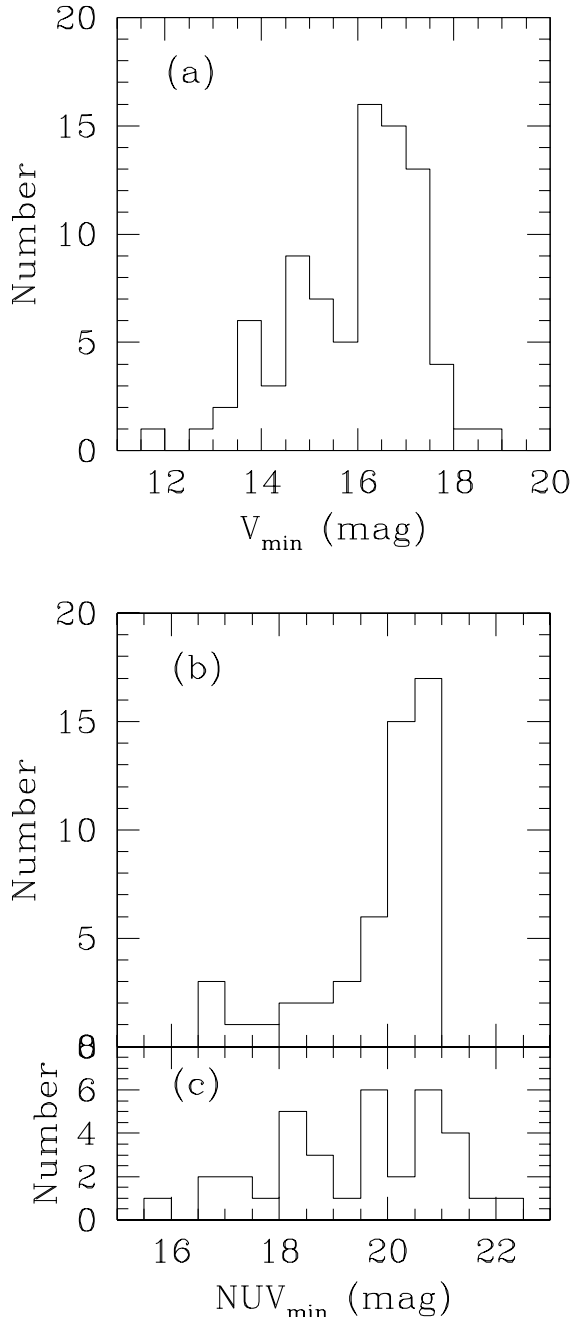


FIG. 10.— The distribution of the RRab in Table 3 versus their  $V$  magnitude at minimum light (panel a). The distribution versus ( $NUV$ ) magnitude at minimum light for Catalog 2 (panel b) and Catalog 1 (panel c).

that the correction for interstellar extinction is small,  $E(B - V) \leq 0.04$  for which  $E(NUV - V) \leq 0.23$ .

The mean  $(NUV - V)$  for RRc is somewhat smaller than that of the RRab, and they have lower amplitudes. Consequently, RRc stars will have a fainter  $V$  magnitude for a given  $NUV$ , and their identification will necessarily be less complete than for the RRab. The  $NUV$  light curve minima in the Gezari catalog are all fainter than 20.0 and so, neglecting extinction, the RRc will have  $V > 17$  and will generally be less easy to detect with existing optical data without the use of new techniques.

The 17 RRc and 48 RRab corresponds to  $\sim 0.40$  vari-

ables per square degree for Catalog 2. This is comparable to the 0.455 RR Lyrae per square degree found by Abbas et al. (2014) in a survey of somewhat greater depth (28 kpc) and which they find has a completeness of  $\sim 50\%$ . This suggests that *GALEX* has detected only half of the RRab to  $V=17.5$ , or else Catalog 2 is itself only about half complete for these variables.

Catalog 2 contains the variables whose  $NUV$  amplitudes are greater or equal to 0.6 mag. The survey covered 169 fields; each field (radius  $0.^\circ 55$ ) was visited from between 10 and 187 times. Table 4 shows that that variables were only discovered in about 20% of the fields when the number of visits was 20 or less but this percentage rose to about 40% when there were over 30 visits. The field centered on AE Aqr is also in the well studied SDSS Stripe 82; three RRc and 2 RRab were found in this field but three RRc of comparable brightness that lie within this field were missed. There were 31 visits to this field but the number of actual detections of the RRc variables ranged from 19 for a 13th mag star to 5 for one at 17th mag. Thus the completeness will vary from field to field depending on the number of visits. In the 19 fields that were visited more than 50 times, eleven RR Lyrae variables were found and only two were missed. It is therefore only in these fields (that comprise only 11% of the total) that the Catalog 2 survey is reasonably complete.

#### 4.5. Contact Binaries.

Contact binaries can be confused with RRc variables that have half their periods; see discussions by Kinman & Brown (2010) and Drake et al. (2014). Table 2 in the appendix (Sec. B) gives the  $UV$  colors for a sample of bright contact binaries and these are plotted against period in Fig. 11.

Drake et al. (2014) use a variety of parameters to distinguish between RRc and contact binaries and conclude that misidentification is most likely to occur among the longer-period bluer contact binaries which are the brightest among such variables; misidentification is therefore not a serious problem for faint surveys. Misidentification apart, the cause of the spread in  $(NUV - V)_0$  among contact binaries needs further investigation. It is unlikely to be caused by a spread in metallicity because the range of metallicity in these objects is small (Rucinski et al. 2013). The presence of companions is a more likely cause since it is known that multiplicity is very common among contact binaries (Pribulla & Rucinski 2008). Smith et al. (2014) consider the effect of companion stars on *GALEX* colors in their discussion of stars in the Kepler field.  $(NUV - V)_0$  may therefore be a useful diagnostic in searching for such companion stars.

#### 4.6. Uncertainties in determining Variable Type and Period.

Five of our new variables (Table 2) are also found in a new catalogue of periodic variables from the Catalina Surveys (Drake et al. 2014, hereafter D14). The first star is J022121.9-033040.0, for which D14 find the same variable type and period as we do. Thus we do not discuss this star further. For the other four stars, we obtain repeat periodograms using the Lomb-Scargle (LS) and Plavchan (PL) routines in the NASA Exoplanet Archive

TABLE 4  
DISCOVERY RATE OF RR LYRAE STARS AS A FUNCTION OF NUMBER OF VISITS PER FIELD FOR CATALOG 2.

| Visits per Field<br>(1) | No. of Fields with this<br>range of visits<br>(2) | Number of Fields in which<br>variables were found<br>(3) |
|-------------------------|---|--|
| 10 to 20                | 86  | 18   |
| 21 to 30                | 39  | 14   |
| 31 to 50                | 25  | 11   |
| > 51                    | 19  | 8  |

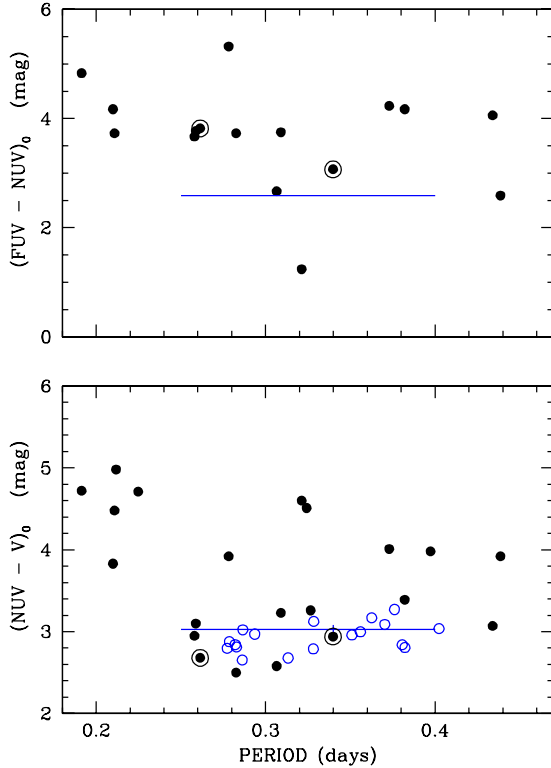


FIG. 11.—  $(FUV - NUV)_0$  (upper panel) and  $(NUV - V)_0$  (lower panel) plotted against the half-periods of a sample of bright contact binaries (black filled circles). Two of these objects (SW Ret and v1643 Sgr) that are shown encircled, are actually RRc variables. The blue horizontal lines in both figures show the location of RRc variables. Our program RRc variables are plotted as blue filled circles using the full periods in the lower figure.

Periodogram Service. Fig. 12 presents the light curves for these four variables. For each variable, the left-hand panel plots the data folded on our period, and the right-hand panel plots the data folded on the D14 period.

With the exception of J154550.8-124936.8, identifying the correct period and type by visual inspection is difficult because of period alias uncertainties. The discrepant results described below illustrate the difficulty in identifying the nature of low-amplitude variables.

J022411.7-052501.6. We identify this as an Algol variable with a period of 0.8254050 days. D14 give the same type with a period of 0.583802 days. The LS routine gives neither of these periods. The PL routine gives both periods; the D14 period has more power in the PL routine and is likely correct.

J122837.9-064230.0. We identify this as an RRab with a period of 0.501648 days. D14 give the same type with a period of 0.333755 days, but call this period “inexact.”

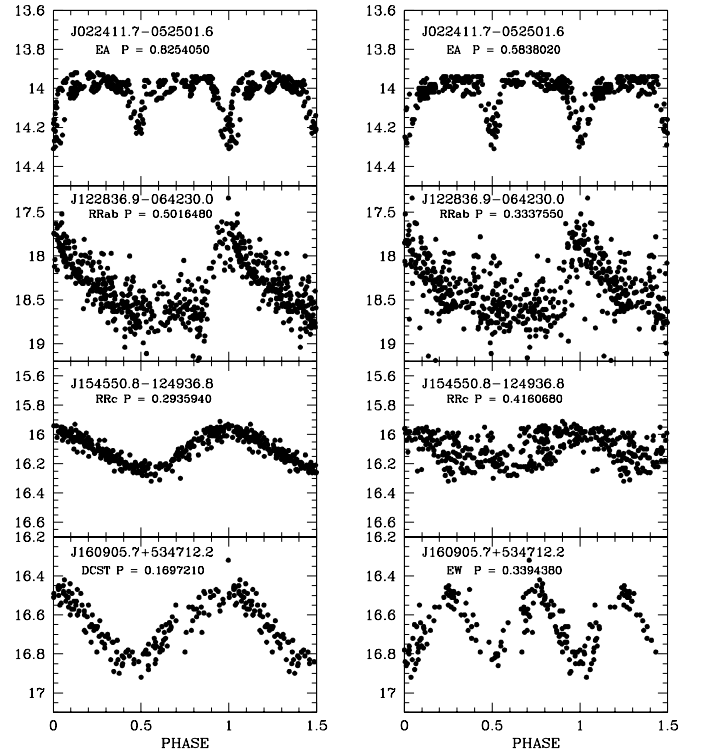


FIG. 12.— Comparison of the light-curves of J022411.7-052501.6, J122837.9-064230.0, J154550.8-124936.8 and 160905.7+534712.2 obtained in this paper (on the left) and those given by Drake et al. (2014) on the right.

The LS and PL routines give both periods, however our period has more power and is likely correct.

J154550.8-124936.8. We identify this as an RRc with a period of 0.293594 days. D14 give the same type with a period of 0.416068 days. Both the LS and PL routines give more power to our period than to the one at 0.416 days, and our period gives a better looking light curve (Fig. 12).

J160905.7+534712.2. We identify this as a  $\delta$  Scuti with a period of 0.1697210 days. D14 identify it with an EW with a period of 0.339438 days. The LP routine gives our period. The PL routine gives both periods with marginally more power to our period. However, the D14 identification is likely correct because the  $(g - r) = 0.32$  color of the variable is probably too red for a  $\delta$  Scuti.

## 5. SUMMARY

We make as complete an identification as possible of unclassified variable stars in existing *GALEX* variable source catalogs. We present newly identified  $\delta$  Scuti, RRc and RRab stars found in what we refer to as Catalog

1 (Welsh et al. 2005) and Catalog 2 (Wheatley et al., 2008). We also examine the sources identified either as “stars” or RR Lyrae stars in the larger catalog of variable *GALEX* sources of Gezari et al. (2013).

We identify 8  $\delta$  Scuti stars, 17 RRc stars, 1 RRd star and 84 RRab stars in Catalogs 1 and 2. These 110 pulsating variables account for 22% of the sources in these Catalogs. Sixteen of these variables were not previously known; their ephemerides and light curves are given in Table 2 and Figures 1, 2, 3 and 4 respectively.

In Table 3 we present new classifications and period measurements for 28 of the 38 variable *GALEX* sources that Gezari et al (2013) identify as RR Lyrae stars: 16 are RRab stars, 4 are RRc stars, 6 are  $\delta$  Scuti stars and 2 are eclipsing systems. We also classify 7 of the 17 *GALEX* sources that Gezari et al. identify as “stars”: 1 is a RRab star, 1 is a RRc star and 5 are eclipsing systems. The classification of these objects depends on our ability to recognize their variability type from optical data in the Catalina Surveys Data Release 2. This becomes difficult for low-amplitude variables with  $V > 17.5$ . Thus classifications are less complete for the Gezari catalog because the catalog contains lower amplitude variables ( $NUV$  amplitude  $\geq 0.2$  mag compared with  $\geq 0.6$  mag for Catalog 2). The light-curves of the variables in Table 2 from the Gezari Catalog are given in Figures 1, 2, 3 and 4.

We find that the  $(NUV - V)_0$  color of low metallicity halo RRab stars is smaller than that of the higher-metallicity *disk* RRab stars. The  $NUV$  pulsation amplitude of RR Lyrae stars is roughly twice that of their  $V$  amplitude (as found earlier by Wheatley et al. (2012)). This allows us to detect low-amplitude variables such as J013642.0-062743.1 and J171251.8+185452.4 which have  $V$  amplitudes of 0.25 and 0.38 mag, respectively. A larger number might be found if the Catalogs were more complete. At a rough estimate, the overall completeness of Catalog 2 is similar to that of the catalog of Abbas et al. (2014) which they estimate as 50%. The completeness of Catalog 2 varies from field to field depending on the number of observations made per field.

$(NUV - V)_0$  is more sensitive than optical colors to changes in  $T_{eff}$  (such as those that occur in stellar pulsation). Four stars that have been described in the literature as RHB stars are actually RR Lyrae stars (e.g. BPS CS 22940-070 which is called non-variable by For et al., (2010)). A plot of  $(NUV - V)_0$  against  $T_{eff}$  shows that the metal-poor RHB stars merge into the RR Lyrae at  $T_{eff} \sim 6000$  K which agrees with other estimates of the red edge of the instability gap. Existing surveys such as Afsar et al. (2012) do not show any metal-rich (disk) RHB stars hotter than  $T_{eff} \sim 5200$  K whereas such stars are known in the metal-rich globular cluster 47 Tuc. We suggest that hotter metal-rich RHB stars could be found by deeper surveys.

We find a large range in both  $(NUV - V)_0$  and  $(FUV - NUV)_0$  colors in a sample of bright contact binaries that have twice the periods of RRc stars and which may therefore be confused with them. These  $UV$  colors do not allow a clear distinction between the two types, but may be of value in detecting companions to the contact binaries.

We acknowledge use of the International Variable Star Index (VSX) database operated at AAVSO, Cambridge, MA, USA. Also the LINEAR survey (available on the SkyDOT website) and funded by NASA at MIT Lincoln Laboratory under Air Force Contract FA8721-05-0002. Also the Catalina Surveys (Data Release 2) that is supported by NASA under grant NNG05GF22G and NSF grants AST-0909182 and AST-1313422. We used the VizieR catalogue access tool, CDC, Strasbourg, France. We acknowledge using data from the SDSS funded by the Alfred P. Sloan Foundation, the Participating Institutions, the NSF and the US D.O.E.. We also used the MAST (Multimission Archive at the STSci which is operated for NASA by AURA), the SIMBAD database (operated at the CDS, Strasbourg, France), ADS (the NASA Astrophysics Data System), and the arXiv e-print server. We also used the NASA Exoplanet Archive which is operated by the California Institute of Technology under contract with NASA.

## REFERENCES

- Abbas, M., Grebel, E., Martin, N., Burgett, W. et al., 2014, MNRAS, 441, 1230
- Afsar, M., Sneden, B., For, B.-Q. 2012, AJ, 144, 20
- Avvakumova, E., Malkov, O., Kniazev, A. 2013, AN, 334, 860
- Alfonso-Garzon, J., Domingo, A., Mas-Hesse, J. 2012, in “Interacting Binaries to Exoplanets”, I.A.U. Symposium No. 282, (eds. Mercedes T. Richards, & Ivan Hubeny), Cambridge University Press, p.484
- Behr, B. 2003, ApJS, 149, 101
- Brown, W., Beers, T., Wilhelm, R., Prieto, C. et al. 2008, AJ, 135, 564
- Cacciari, C., Corwin, T., Carney, B., 2005, AJ, 129, 267
- Christlieb, N., Scharck, T., Friebel, A., Beers, T. et al. 2008, A&A, 484, 721
- Corben, P., Carter, B., Banfield, R., Harvey, G. 1972, MNRAS, 31, 7
- Dambis, A., Berdnikov, L., Kniazev, A., Kravtsov, A. et al. 2013, MNRAS, 435, 3206
- Drake, A., Catelan, S., Djorgovski, S., Torrealba, G. et al. 2013, ApJ, 763, 32
- Drake, A., Graham, M., Djorgovski, S., Catelan, S. 2014, ApJS, 213, 9
- Dvorak, S. 2004, IBVS, No. 5549
- Ferro, A., Pena, J., Jaimes, R. 2013. R. Mx. A. A., 49. 43
- Flesch, E. 2010, PASA, 27, 283
- For, B.-Q., Sneden, C., 2010, AJ, 140, 1694
- Gezari, S., Matin, D., Forster, K., Neill, J. et al. 2013, ApJ, 766, 60 (*GALEX* Time Domain Survey)
- Girard, T., van Alena, W., Zacharias, N., Casetti-Dinescu, D. et al. 2011. yCat. 1320. (SPM 4.0 Catalog)
- Hansen, C., Nordstrom, B., Bonifacio, P., Spite, M., et al. 2011, A&A, 527, A65
- Ishigaki, M., Aoki, W., Chiba, M. 2013, ApJ, 771, 67
- Keller, S., Murphy, S., Prior, S., Da Costa, G. et al. 2008, ApJ, 678, 851
- Kinman, T., Salim, S., & Clewley, L. 2007, ApJL, 662, 111
- Kinman, T., Morrison, H., Brown, W. 2009, AJ, 137, 3198
- Kinman, T., Brown, W. 2010, AJ, 139, 2014
- Kinemuchi, K., Smith, H., Woźniak, P. & McKay, T. 2006, AJ, 132, 1202
- Kraus, A., Craine, E., Giampapa, M., Scharlach, W. et al., 2007, AJ, 134, 1488
- Li, Y., Wei, J.-Y., He, X.-T. 2011, Res. Astron. Astrophys., 11, 833
- Malkov, O., Oblak, E., Snegereva, E., Torra, J. 2006, A&A, 446, 785
- Martin, D.C., Fanson, J., Schiminovich, D., Morrissey, P. et al. 2005, ApJL, 619, 1

- Miceli, A., Rest, A., Stubbs, C., Hawley, S. et al. 2008, ApJ, 678, 865
- McNamara, D. 1997, PASP, 109, 1221
- Nichols, J., Henden, A., Huenemoerder, D., Lauer, J. 2010, ApJS, 188, 473
- Norton, A., Wheatley, P., West, R., Haswell, C. et al. 2007, A&A, 467, 785
- Palaversa, L., Ivezić, Eyer, L., Ruzdjak, D. et al. 2013, AJ, 146, 101
- Peek, & Schminovich 2013, ApJ, 771, 68
- Petersen, J., Hog, E. 1998, A&A, 331, 989
- Pojmanski, G. 2002, Acta Astron., 52, 397
- Poleski, R. 2014, PASP, 126, 509
- Preston, G., Schectman, S., Beers, T. 1991, ApJ, 121, 375
- Pribulla, T., Rucinski, S. 2008, “Multiple Stars Across the H-R Diagram”, ESO Astrophysics Symposia, Springer-Verlag, Berlin Heidelberg, p. 163
- Rey, S-C., Rich, R., Sangmo, T., Suk-Yin, Y. et al. 2007, ApJS, 173, 643
- Rucinski, S., Pribulla, T., Budaj, J. 2013, AJ, 146, 70
- Preston, G., Sneden, C., Thompson, I., Shectman, S. et al. 2006, AJ, 132, 85
- Samus, N., Durlevich, O. et al., 2012 (General Catalogue of Variable Stars)
- Schmidt, E. 2002, AJ, 123, 965
- Sesar, B., Ivezić, Z., Grammer, S., Morgan, et al., 2010, ApJ, 708, 717
- Sesar, B., 2012, AJ, 144, 114
- Sesar, B., Ivezić, Z., Sturat, J., Morgan, D., et al. 2013, AJ, 146, 21
- Smith, M., Bianchi, L., Shiao, B. 2014, AJ, 147, 159
- Suvelges, M., Sesar, B., Veradi, M., Mowlavi, N. et al. 2012, MNRAS, 424, 2528
- Szczegiel, D., Fabrycky, D. 2007, MNRAS, 377, 1263
- van Leeuwen, F., 2007, A&A, 474, 653
- Vivas, A., Zinn, R., Abad, C., et al., 2004, AJ, 127, 1158
- Watson, C. 2006, JAVSO, 35, 318 (VSX Catalogue)
- Welsh, B., Wheatley, J., Heafield, K., Seibert, M. et al. 2005, AJ, 130, 825 (The *GALEX* Ultraviolet Variability Catalog)
- Wheatley, J., Welsh, B., Sallman, S., Siegmund, O. 2003, BAAS, 35, 1338
- Wheatley, J., Welsh, B., Browne, S. et al. 2008, AJ, 136, 259 (The Second *GALEX* Ultraviolet Variability Catalog).
- Wheatley, J., Welsh, B., 2012, PASP, 124, 552
- Wils, P., Lloyd, C., Bernhard, K. 2006, MNRAS, 368, 1757
- Wils, P. 2010, AAVSO Variable Star Index (VSX Catalogue)
- Zinn, R., Horowitz, B., Vivas, A., Baltay, C. et al. 2014, ApJ, 781, 22

## APPENDIX

A. HIGH-AMPLITUDE  $\delta$  SCUTI STARS (HADS).

The High-Amplitude  $\delta$  Scuti stars are radially pulsating stars with periods in the range 0.04 to 0.30 days that are largely monoperiodic. They show some overlap in period with the RRc variables but can usually be distinguished from them by having more asymmetric light curves. Table A1 gives the  $(NUV - V)_0$  for a sample of these stars drawn from the compilations of McNamara (1997) and Suveges et al. (2012). The HADS are well separated from the RRc variables in the  $(NUV - V)_0$  vs. Period plot (Fig. 6); this is clearly the case for SS Psc (which is marked in this figure). This is of interest because Ferro et al. (2013) were unable to classify this star from their Stromgren photometry. The revised Hipparcos parallax of SS Psc is  $5.26 \pm 1.99$  (van Leeuwen, 2007) gives an  $M_v$  of between +3.5 and +5.2 which is in the expected range for HADS (Peterson & Hog, 1998).

TABLE 1  
( $NUV - V$ )<sub>0</sub> FOR  $\delta$  SCUTI STARS.

| R.A. <sup>a</sup><br>(deg.)<br>(1) | Dec. <sup>b</sup><br>(deg.)<br>(2) | Ref <sup>c</sup><br>(3) | ( $NUV - V$ ) <sub>0</sub> <sup>d</sup><br>(mag.)<br>(4) | Period <sup>e</sup><br>(days)<br>(5) | GCVS ID <sup>f</sup><br>(6) |
|------------------------------------|------------------------------------|-------------------------|--|--------------------------------------|-----------------------------|
| 144.2216                           | +44.0668                           | 1                       | 3.330  | 0.0860100                            | AE UMa                      |
| 231.0294                           | +36.8670                           | 1                       | 3.118  | 0.1040900                            | YZ Boo                      |
| 238.2908                           | +06.0907                           | 1                       | 3.193  | 0.1891500                            | CW Ser                      |
| 013.8256                           | +23.1637                           | 1                       | 2.461  | 0.0786800                            | GP And                      |
| 337.5121                           | -08.1075                           | 1                       | 3.912  | 0.1683800                            | GV Aqr                      |
| 247.8249                           | +11.9979                           | 1                       | 3.392  | 0.1486300                            | DY Her                      |
| 247.5682                           | +16.9185                           | 1                       | 2.550  | 0.0946800                            | v1116 Her                   |
| 357.1914                           | -08.1457                           | 1                       | 3.767  | 0.1978230                            | BS Aqr                      |
| 146.4452                           | -12.9940                           | 1                       | 3.226  | 0.2233891                            | VX Hya                      |
| 020.2182                           | +21.7287                           | 1                       | 3.898  | 0.2877928                            | SS Psc                      |
| 270.6644                           | +62.7186                           | 2                       | 3.393  | 0.1969000                            | v395 Dra                    |
| 278.0269                           | +40.5991                           | 2                       | 2.790  | 0.1021400                            | v593 Lyr                    |
| 240.7758                           | +26.2396                           | 2                       | 4.357  | 0.1924460                            | BY CrB                      |
| 237.4137                           | -76.4219                           | 2                       | 2.182  | 0.0638630                            | v360 Aps                    |
| 343.0172                           | -0.8690                            | 3                       | 3.214  | 0.0495655                            |                             |
| 320.2203                           | +0.2755                            | 3                       | 2.067  | 0.0500164                            |                             |
| 319.3871                           | +0.8267                            | 3                       | 2.813  | 0.0493681                            |                             |
| 318.9853                           | -0.8594                            | 3                       | 2.472  | 0.0512525                            |                             |
| 044.3292                           | -0.6536                            | 3                       | 2.323  | 0.0482597                            |                             |
| 037.4992                           | +1.2482                            | 3                       | 2.380  | 0.0509957                            |                             |
| 341.6031                           | +1.1892                            | 3                       | 2.754  | 0.0502367                            |                             |
| 338.5538                           | +0.7835                            | 3                       | 2.794  | 0.0537832                            |                             |
| 322.4356                           | +1.0480                            | 3                       | 2.421  | 0.0596027                            |                             |
| 320.6782                           | +0.7816                            | 3                       | 2.386  | 0.0538881                            |                             |
| 313.7465                           | -0.1246                            | 3                       | 2.024  | 0.0515025                            |                             |
| 312.4206                           | -0.3539                            | 3                       | 2.749  | 0.0931453                            |                             |
| 322.4695                           | -1.1719                            | 3                       | 2.989  | 0.0805862                            |                             |
| 321.1715                           | +0.0444                            | 3                       | 2.451  | 0.0452487                            |                             |
| 043.1488                           | +0.2955                            | 3                       | 2.480  | 0.0550160                            |                             |
| 355.3285                           | +0.7152                            | 3                       | 3.247  | 0.1198865                            |                             |
| 323.7998                           | +0.6225                            | 3                       | 2.782  | 0.0872579                            |                             |
| 313.1301                           | -0.5333                            | 3                       | 2.554  | 0.0530346                            |                             |
| 305.7112                           | -0.1257                            | 3                       | 2.468  | 0.0521552                            |                             |
| 320.1692                           | +0.9076                            | 3                       | 1.698  | 0.0742401                            |                             |
| 316.8586                           | +1.1715                            | 3                       | 3.410  | 0.0678054                            |                             |
| 310.7717                           | +0.0367                            | 3                       | 2.386  | 0.0457611                            |                             |
| 310.3194                           | +0.5634                            | 3                       | 2.739  | 0.0663556                            |                             |
| 357.0749                           | +0.9069                            | 3                       | 2.562  | 0.0607696                            |                             |
| 314.2421                           | +1.0685                            | 3                       | 2.722  | 0.0702984                            |                             |
| 304.6618                           | +1.0123                            | 3                       | 3.566  | 0.0457270                            |                             |
| 346.1327                           | +0.4127                            | 3                       | 2.390  | 0.0565413                            |                             |
| 002.3078                           | -0.1846                            | 3                       | 2.426  | 0.0519909                            |                             |
| 338.6537                           | +0.3735                            | 3                       | 2.625  | 0.0530301                            |                             |
| 320.8264                           | +0.8867                            | 3                       | 2.186  | 0.0706932                            |                             |
| 045.7345                           | -0.6974                            | 3                       | 2.804  | 0.0581344                            |                             |

REFERENCES. — (1) McNamara (1997); (2) Samus et al. (2012), (General Catalogue of Variable Stars); (3) Suveges et al. (2012).

<sup>a</sup> Right Ascension in decimal degrees.

<sup>b</sup> Declination in decimal degrees.

<sup>c</sup> Reference for identification as  $\delta$  Scuti star.

<sup>d</sup> Dereddened difference between mean  $NUV$  and  $V$  magnitudes.

<sup>e</sup> Period in days.

<sup>f</sup> Identification in General Catalogue of Variable Stars.

TABLE 2  
UV COLORS FOR BRIGHT CONTACT BINARIES.

| R.A. <sup>a</sup><br>(deg.)<br>(1) | Dec. <sup>b</sup><br>(deg.)<br>(2) | b <sup>c</sup><br>(deg.)<br>(3) | $(NUV - V)_0$ <sup>d</sup><br>(mag.)<br>(4) | $(FUV - NUV)_0$ <sup>e</sup><br>(mag)<br>(5) | X-ray <sup>f</sup><br>(6) | $P_{0.5}$ <sup>g</sup><br>(days)<br>(7) | GCVS ID <sup>h</sup><br>(8) |
|------------------------------------|------------------------------------|---------------------------------|---|--|---------------------------|---|-----------------------------|
| 130.0071                           | +18.9998                           | +32.17                          | 4.72  | 4.83   | X                         | 0.1914                                  | TX Cnc                      |
| 150.6998                           | +01.0945                           | +41.94                          | 3.83  | 4.17   | ...                       | 0.2099                                  | Y Sex                       |
| 258.4909                           | +16.3502                           | +28.73                          | 4.48  | 3.73   | X                         | 0.2108                                  | AK Her                      |
| 077.8104                           | -08.5569                           | -26.13                          | 4.98  | ...  | X                         | 0.2117                                  | ER Ori                      |
| 141.6710                           | -13.7518                           | +25.68                          | 4.71  | ...  | ...                       | 0.2248                                  | EZ Hya                      |
| 234.1083                           | +15.5317                           | +50.1                           | 2.95  | 3.67   | ...                       | 0.2580                                  | CC Ser                      |
| 299.2000                           | +01.1000                           | -14.0                           | 3.10  | 3.77   | ...                       | 0.2588                                  | v0724 Aql                   |
| 052.0838                           | -64.9772                           | -44.8                           | 2.68  | 3.82   | ...                       | 0.2614                                  | SW Ret†                     |
| 126.1351                           | -16.4032                           | +12.04                          | 3.92  | 5.32   | ...                       | 0.2782                                  | AV Pup                      |
| 079.9754                           | -35.9017                           | -33.2                           | 2.50  | 3.73   | ...                       | 0.2826                                  | RZ Col                      |
| 354.8175                           | -09.1534                           | -65.2                           | 2.58  | 2.67   | ...                       | 0.3065                                  | EK Aqr                      |
| 160.1383                           | +13.5669                           | +56.59                          | 3.23  | 3.75   | ...                       | 0.3090                                  | UZ Leo                      |
| 180.2646                           | +13.0083                           | +71.61                          | 4.60  | 1.24   | ...                       | 0.3213                                  | AG Vir                      |
| 143.0766                           | -28.6278                           | +16.61                          | 4.51  | ...  | ...                       | 0.3242                                  | S Ant                       |
| 277.4200                           | +31.0003                           | +17.9                           | 3.26  | ...  | ...                       | 0.3266                                  | IY Lyr                      |
| 296.4417                           | -40.9383                           | -27.3                           | 2.94  | 3.07   | ...                       | 0.3398                                  | v1643 Sgr†                  |
| 212.3643                           | -15.5816                           | +43.3                           | 4.01  | 4.23   | ...                       | 0.3730                                  | CX Vir                      |
| 119.5459                           | +72.7643                           | +30.7                           | 3.39  | 4.17   | ...                       | 0.3821                                  | CD Cam                      |
| 311.6156                           | -71.9495                           | -34.5                           | 3.98  | ...  | ...                       | 0.3974                                  | MW Pav                      |
| 274.2226                           | +27.6628                           | +19.3                           | 3.07  | 4.06   | ...                       | 0.4340                                  | MS Her                      |
| 252.3800                           | +47.1080                           | +39.9                           | 3.92  | 2.59   | ...                       | 0.4386                                  | v921 Her                    |

NOTE. — † Both SW Ret and v1643 Sgr are RR Lyrae stars.

<sup>a</sup> Right Ascension in decimal degrees.

<sup>b</sup> Declination in decimal degrees.

<sup>c</sup> Galactic Latitude.

<sup>d</sup> Dereddened difference between mean  $NUV$  and  $V$  magnitudes.

<sup>e</sup> Dereddened difference between mean  $FUV$  and  $NUV$  magnitudes.

<sup>f</sup> Given as X-ray source by Flesch (2010).

<sup>g</sup> Half of period in days.

<sup>h</sup> Identification in General Catalogue of Variable Stars.

## B. CONTACT BINARIES

Table A2 gives the  $(NUV - V)_0$  and  $(FUV - NUV)_0$  for a sample of bright contact binaries with half-periods between 0.19 and 0.44 days (primarily taken from Malkov et al., 2006). We excluded variables at low galactic latitudes ( $|b| < 14^\circ$ ) in order to minimize errors in the corrections for extinction. The extinction correction used to derive  $(FUV - NUV)_0$  is less than that for  $(NUV - V)_0$ , but  $FUV$  is available for fewer stars. The data from Table A2 is plotted in Fig. 11.

The  $(NUV - V)_0$  of the 17 RRc that we found in Catalogs 1 and 2 range from 2.65 to 3.17 ( $\sigma = 0.14$  mag) while in a sample of 50 RRc from the Abbas et al. catalog, the range is from 2.36 to 3.52 ( $\sigma = 0.26$  mag). The *mean*  $NUV$  in the former case were derived from multiple values of  $NUV$  whereas in the latter case only a single value was usually available; this may well explain the greater spread of  $(NUV - V)_0$  found for the RRc in the Abbas et al. catalog.

Half the contact binaries in Table A2 have  $(NUV - V)_0$  within the range that we find for the RRc. Two of these stars with low  $(NUV - V)_0$  are actually RR Lyrae stars: SW Ret is an RRd (Szcziel & Fabrycky 2007) and v1643 Sgr is an RRc (Dvorak 2004). The more recent catalog of Avvakumova et al. (2013) continues to identify v1643 Sgr as a contact binary. The mean  $(FUV - NUV)_0$  of 16 RRc variables is  $+2.59 \pm 0.14$ . In Table A2, EK Aqr, AG Vir, v941 Her and the RRc v1643 Sgr are within the range of  $(FUV - NUV)_0$  occupied by RR Lyraes; AG Vir is known to have an infra-red excess (Nichols et al. 2010).

## C. RED HORIZONTAL BRANCH (RHB) STARS.

Fig. 9 (Sec. 4.3) shows the trend of  $(NUV - V)_0$  with effective temperature ( $T_{eff}$ ) for RHB stars in three metallicity ( $[Fe/H]$ ) ranges. The data used in this plot are given in Table A3. We take all stars with the type RHB in Table 2 of Behr (2003), and we also take NSV 4256 (HD 82590), which Behr lists as RR?, because its  $T_{eff}$  (6094 K) is near the red edge of the instability gap. The classification of NSV 4256 is uncertain but it is likely to be one of the lowest amplitude RR Lyrae stars known; both Corben et al. (1972) and Alfonzo-Garzon et al. (2012) give NSV 4256 a  $V$  amplitude of 0.06 mag. Further data were taken from: Preston et al. (2006), For & Sneden (2010) and Afsar et al. (2012). We expect that errors in  $T_{eff}$  are about  $\pm 150$  K. To illustrate this uncertainty, we provide data for HD 119516 from two different sources in Table A3, and plot the points separately (joined by a dotted line) in Fig. 9.

Behr (2003) place the red edge of the instability strip at  $T_{eff}=6000$  K (as plotted in Fig. 9). Preston et al. (2006) and For & Sneden (2010) give  $6310 \pm 145$  K and 5900 K, respectively, for this quantity. These temperatures are appropriate for the lowest metallicity stars (plotted in green in Fig 5.). Bearing in mind the uncertainties in  $T_{eff}$ , these estimates for the red edge of the instability strip are in reasonable agreement with our data. We find that  $(NUV - V)_0$  increases with increasing metallicity at a given  $T_{eff}$ .

There is, however, a large gap in  $T_{eff}$  between the hottest metal-rich RHB stars that we have found in the literature and the  $T_{eff}$  of the metal-rich disk RR Lyrae stars. We estimate the latter to have  $T_{eff} \geq 6500$  K based on the  $(V - K)$  of a small sample of these stars. The blue tip of red horizontal branch of the metal-rich globular cluster 47 Tuc (Salaris et al. 2007) has  $J - K \sim 0.40$  to 0.45, whereas the hottest of our metal-rich RHB stars has  $J - K = 0.53$ . We therefore suspect that the lack of hotter stars among our sample of metal-rich RHB stars is an observational selection effect. The faintest 15 of the 76 stars studied by Afsar et al. (2012) have  $V$  between 9.0 and 10.5, which for  $M_v = +0.8$  corresponds to distances between 436 and 870 pc. Thus, as they point out, their sample strongly favors thin disk stars. A search for thick disk RHB stars must be made at significantly fainter magnitudes.



TABLE 3  
 $(NUV - V)_0$ ,  $[\text{Fe}/\text{H}]$  AND  $T_{\text{eff}}$  FOR A SAMPLE OF RHB STARS.

| Identification   | $(NUV - V)_0$ <sup>a</sup><br>mag. | $[\text{Fe}/\text{H}]$ | $T_{\text{eff}}$<br>deg K | Ref.   | Notes |
|------------------|------------------------------------|------------------------|---------------------------|--------|-------|
| (1)              | (2)                                | (3)                    | (4)                       | (5)    | (6)   |
| HIP 62325        | 8.117                              | -0.06                  | 4710                      | (6)    |       |
| BD 25°2459       | 7.101                              | -0.28                  | 4743                      | (1)    |       |
| HIP 115839       | 6.285                              | -0.40                  | 5000                      | (6)    |       |
| BD 34°2371       | 7.262                              | -0.41                  | 5005                      | (1)    |       |
| HIP 3031         | 8.058                              | -0.53                  | 5020                      | (6)    |       |
| BD 29°2294       | 6.411                              | -0.55                  | 5132                      | (1)    |       |
| BD 29°2231       | 7.076                              | -0.65                  | 4756                      | (1)    |       |
| HIP 45412        | 6.870                              | -0.68                  | 5080                      | (6)    |       |
| BD 25°2436       | 7.041                              | -0.76                  | 4847                      | (1)    |       |
| BD 36°2303       | 7.860                              | -0.77                  | 4705                      | (1)    |       |
| HIP 5104         | 6.335                              | -0.86                  | 5100                      | (6)    |       |
| HD 110930        | 6.854                              | -0.94                  | 4934                      | (1)    |       |
| HIP 4960         | 5.516                              | -1.02                  | 5260                      | (6)    |       |
| HD 112030        | 7.111                              | -1.12                  | 4699                      | (1)    |       |
| HD 202573        | 6.706                              | -1.21                  | 4853                      | (1)    |       |
| BD 27°2057       | 7.246                              | -1.25                  | 4695                      | (1)    |       |
| HD 6229          | 5.516                              | -1.35                  | 5200                      | (1)    |       |
| HD 97            | 5.678                              | -1.42                  | 5272                      | (1)    |       |
| BPS CS 22940-070 | 3.024                              | -1.47                  | 6100                      | (2)    | (1)   |
| HD 82590         | 3.893                              | -1.50                  | 6094                      | (1)    | (2)   |
| HD 105546        | 5.437                              | -1.67                  | 5299                      | (1)    |       |
| HD 63791         | 6.735                              | -1.72                  | 4954                      | (1)    |       |
| BD 18°2890       | 5.334                              | -1.78                  | 5347                      | (1)    |       |
| HD 119516        | 4.224                              | -1.92                  | 5689                      | (1)(4) |       |
| BD 10°2495       | 5.040                              | -2.07                  | 5275                      | (1)    |       |
| BD 17°3248       | 4.480                              | -2.08                  | 5398                      | (1)    |       |
| BPS CS 22886-043 | 3.631                              | -2.15                  | 6000                      | (2)    |       |
| HD 119516        | 4.233                              | -2.16                  | 5400                      | (3)    |       |
| BPS CS 22888-047 | 3.487                              | -2.35                  | 6000                      | (2)    | (3)   |
| BD 18°2757       | 5.527                              | -2.43                  | 4741                      | (1)    |       |
| BPS CS 22882-001 | 3.483                              | -2.54                  | 5950                      | (3)    |       |
| BPS CS 22875-029 | 3.391                              | -2.66                  | 6000                      | (3)    |       |
| BPS CS 22191-029 | 3.417                              | -2.72                  | 6000                      | (3)    |       |
| BPS CS 22881.039 | 3.178                              | -2.73                  | 6100                      | (3)    | (4)   |
| BPS CS 22186-005 | 3.318                              | -2.77                  | 6200                      | (3)    | (5)   |
| BPS CS 30317-056 | 3.441                              | -2.85                  | 6000                      | (5)    | (6)   |

REFERENCES. — (1) Behr (2003); (2) Preston et al. (2006); (3) For & Sneden (2010). (4) Ishigaki et al. (2013); (5) Hansen et al. (2011). (6) Afsar et al. (2012).

NOTE. — (1) RRab variable; Period = 0.5103 days;  $V_{\text{amp}} \sim 0.9$  mag. (this paper) (2) NSV 4526;  $V_{\text{amp}} \sim 0.06$  mag. (Corben et al. 1972; Alfonso-Garzon et al. , 2012); type uncertain. (3)  $[\text{C}/\text{Fe}] = 1.4$  (Christlieb et al., 2008). (4) RRab variable, Period = 0.66876 days;  $V_{\text{amp}} \sim 0.8$  mag. (Hansen et al., 2011);  $[\text{C}/\text{Fe}] = 2.0$  (Christlieb et al., 2008) (5)  $[\text{C}/\text{Fe}] = +1.0$  (Christlieb et al., 2008) (6) RRab variable, Period = 0.74851 days;  $V_{\text{amp}} \sim 0.35$  mag. (Hansen et al., 2011)

<sup>a</sup> Dereddened difference between mean  $NUV$  and  $V$  magnitudes.